Safety in Mines Research Advisory Committee

Final Project Report

Interaction between stope support and ground motion in the hangingwall and footwall

Project Leader : Dr A Cichowicz

Research agency : ISS International Limited

Project number : GAP845

Project duration : April 2001 to Mar 2002

Report date : July 2002

Document number : GAP845-REP-004

Executive Summary

The observed and theoretical responses of timber packs were analyzed. A set of data collected from Mponeng Mine provides an insight into the response of support units under seismic load. The most important accomplishment of monitoring is the measurement of strong ground motion in the hangingwall, footwall and support units. The strongest monitored ground motion was caused by an event of magnitude 1.8 at a distance of less than 40 m with a peak ground acceleration, PGA, of 170m/s^2, a peak ground velocity, PGV, of 1.2 m/s and the final displacement was 31 mm.

This report describes the dynamic behavior of stope support. To predict deformation of the support under seismic load a reasonable model of support was developed. It is assumed that the response of the stope support can be adequately simulated using a one-degree-of-freedom system, SDOF. The SDOF model was developed for support under multiple excitations. The dynamic response of a support was solved using numerical methods. The proposed model was applied to the data, its advantages and limitations were verified by detailed testing with the strong ground motion data. The support response may be simulated using SDOF model when PGA is in the range 18 - 100 m/s^2 ; for this data model shows that the maximal value of the stiffness is 120,000 kN/m and it is associated with a relatively small deformation of 1 mm measured at the center of support and the very large viscous damping attenuation. The ground motion caused elastic deformation, however, a small inelastic component of the motion could be introduced as well.

The ground motion with peak ground PGV = 1.2 m/s is responsible for permanent deformation of 23.6 mm in the upper part of support and the maximal reaction force acting at the top of support is 950-1400 kN. The data show that the timber pack does not deform as one uniform block. The difference in ground motion between the hangingwall and footwall has an effect on the way the pack is deformed. The equation governing the model with two or three degrees of freedom with multiple excitation was developed.

The theoretical basis for the estimation of energy absorbed by a support unit using data recorded in the support unit, hangingwall and footwall was given. The damping and yielding influence the manner in which energy is dissipated. The energy is dissipated by viscous damping in the elastic system and by viscous damping and yielding in the inelastic system. The values of the kinetic and strain energy are generally small compared to the damping and hysteretic energies at the end of the record.

The response of the support to strong ground motion has radically different characteristics in comparison to its response to weak ground motion. Therefore, parameters of weak ground motion cannot be used as an indicator of support behavior under strong ground motion as they are quantitatively different. A simple scaling law is not applicable. The PGV and PGA are not the best parameters for measuring the input energy to the support. The full waveform should be studied instead.

Acknowledgements

Site selection and data collection would have been impossible without help from Mr A. Ward of Mponeng Mine.

Table of contents

List of figures

Figure 3.10c Estimates of the displacement differences between the layers of the support.

Figure 4.1 Support model - a 3-degree-of-freedom system subjected to the hangingwall u_0 and the footwall u_4 motion.

Figure 4.2 Support model - a 2-degree-of-freedom system subjected to the hangingwall u_0 and the footwall u_3 motion.

Figure 4.3 Support model - a one-degree-of-freedom system subjected to the hangingwall, $u_o = u_h$, and the footwall, $u_2 = u_f$ motion.

Figure 4.4 Schematic of deformation under load, where a support is exposed to deformation caused by the stope closure and seismic load. Two simple examples of seismic deformation are imposed on long term deformation. The first seismic event does not lead to permanent elastic deformation and the second event with stronger amplitude induced a permanent deformation, Δu . The two seismic loads are applied only for a short time.

Figure. 4.5 The bilinear hysteretic load deformation model. k_1, is the initial elastic stiffness, k_2 is the stiffness after yielding, u_y is the yielding displacement (displacement related to point B).

Figure 4.6 A comparison between the observed velocity motion of the middle of the support and the velocity of motion imposed by the loading (top). Magnitude 1.1, January 31 2002, 00:08:38hr (bottom). Seismic event with magnitude 1.8 November 22 2001, 21:12:03hr

Figure 4.7 A Response of the timber pack to ground motion. The motion of the middle of the support , $v_m(t)$, $a_m(t)$, and the relative motion of the middle of the support $v_r(t)$ $a_r(t)$ for the initial pulse and the whole waveforms are shown. The first pulse is modeled using k_1=30,000 kN/m, β= 0.3 The solid line represents theoretical acceleration and velocity, the dotted line is for the observed one. Data for the seismic event with magnitude 1.1 Mponeng Mine January,31, 2002, 00:02hr

Figure 4.7 B The whole record is modeled using k_1=100,000 kN/m, β =0.6.

Figure 4.8 Response of the timber pack to the ground motion. The motion of the middle of the support , $v_m(t)$, $a_m(t)$, and the relative motion of the middle of the support $v_r(t)$ $a_r(t)$ for the whole waveforms are shown. The whole record is modeled using k_1=100,000 kN/m, β =0.8, f_y = 15000 N and stiffness after linear deformation, k_2=0.5 k_1. The solid black line represents a theoretical acceleration and velocity, the dotted line is for the observed ones. Data for the seismic event magnitude 1.1 Mponeng Mine January 31, 2002, 00:02hr

Figure 4.9.A The reaction force, f_s ($u_{r,}$,v_r), versus displacement and the reaction force

plus damping force, $f_s(u_{r,,}v_r) + f_d(v_r)$, versus displacement for the event analyzed in Figure 4.7. The whole record is modeled using k_1=100,000 kN/m, β =0.8, f_y = 15000 N and stiffness after linear deformation, k_2=0.5 k_1 Data for the seismic event with magnitude 1.1, Mponeng Mine January31, 2002, 00:02hr

Figure 4.9.B The reaction force, $f_s(u_{r,,}v_r)$, versus displacement and the reaction force plus damping force, $f_s(u_{r,,}v_r) + f_d(v_r)$, versus displacement for the event analyzed in Figure 4.7. The whole record is modeled using k_1=15,000 kN/m, β =0.3, f_y = 5000 N and stiffness after linear deformation, k_2=0.5 k_1 Data for the seismic event with magnitude 1.1, Mponeng Mine January31, 2002, 00:02hr

Figure 5.1 Time variation of energy dissipated by viscous damping and kinetic plus strain energy. Seismic event with magnitude 1.1 January 31, 2002, 00:02hr.

Figure 5.2 A Time variation of energy dissipated by viscous damping and yielding and kinetic plus strain energy. The whole record is modeled using k_1=100,000 kN/m, β =0.8, f_y = 15000 N and stiffness after linear deformation, k_2=0.5 k_1 Data for the seismic event with magnitude 1.1, Mponeng Mine January31, 2002, 00:02hr

Figure 5.2 B Time variation of energy dissipated by viscous damping and yielding and kinetic plus strain energy. The whole record is modeled using k_1=15,000 kN/m, β =0.3, f_y = 5000 N and stiffness after linear deformation, k_2=0.5 k_1 Data for the seismic event with magnitude 1.1, Mponeng Mine January31, 2002, 00:02hr

List of tables

Table 3.1 Differences of the ground motion parameters in the layers of the support for the event of magnitude 1.8 less than 40m distant from the array of sensors

1 Introduction

The primary output of this project is an analysis of the relationships between ground motion recorded at the walls of a stope and in the stope support. The project consists of the following two enabling outputs

1 Data base of ground motion at the surface of a stope
2 Stope support response to strong ground motion.

The structure of the report follows the methodology outlined in the proposal. Chapter 2 addresses the first enabling output. The rest of the report follows the research objective outlined in the primary output and the methodology of the proposal. The analysis addresses the following problems:

- Study of waveforms recorded in stope support and ground motion in the hangingwall and footwall.

- Modelling of load deformation during cyclic seismic loading.

- Estimation of energy absorbed by support units during strong ground motion

Generally, we have to acquire some knowledge that will allow us to predict support response caused by a known ground motion of the footwall and hangingwall. The ultimate goal of the research is to set parameters for the design of support that will control energy distributed per cycle of deformation.

2 Data Base Description and Logistic Issues

An experiment was conducted at several sites near a stope face in Mponeng Mine. The data base has a few hundred seismic events recorded by six vertical accelerometers, QS, installed on the surfaces of hangingwall, footwall and stope support. Seismic sensors were installed near the pack and in the pack itself. More than 50 events have a peak ground acceleration (PGA) larger than 10 m/s^2. Some 26 events with the strongest ground motion were selected for detailed analysis. The project GAP845 is a continuation of work from the project GAP709b.

During the period of July through September 2001 data were collected from Mponeng mine. However, there were several disruptions in monitoring. Initially, two sets of recording instruments (RS) were installed, each one with three vertical accelerometers. On August 10, 24 and 31 the RS had falls of ground close by and sensors were damaged.

After the repairs have been done, the RS were re-installed. On September 14 we found out that the RS had been backfilled. Finally, one RS and one set of sensors were recovered. Despite these logistic difficulties we had a few days of good monitoring in July and September.

To help the project, ISSI allocated a new generation of data acquisition unit, a QS. The unit has six vertical channels. In the initial phase both the RS and QS were used to monitor ground motion in the stope.

During the period of October through December 2001 a new site was established in section 121, panel East 7 crosscut 44 level 99, 25 m from the face. During December the QS battery charger did not work properly.

In the initial stage the QS was installed in the backfill area. The sensors were attached to the footwall and the hangingwall. A seismic event with magnitude 2.9 was located some 100 m from the site. After recording this strong ground motion, the QS station was moved to the next site. The site was located 10 m away from the face next to the gully. The dynamic response of a timber pack (mat pack) with sides 1.5m by 1.5m and height 1.3m was monitored.

Six QS vertical accelerometers were installed as follows: sensor 1 was on the footwall, sensor 2 on the pack, 25 cm from the footwall, sensor 3 was in the centre of the pack, sensor 4 was 25 cm from the hangingwall, sensor 5 was attached to the hangingwall next to pack, sensor 6 was attached to the hangingwall, 1 m from the pack. At this site the QS recorded several events with peak ground acceleration larger than 100m/s^2.

When the level of seismicity dropped, the experiment was moved to a new site to be closer to an active exploitation. During the period from 15 February to 15 March 2002 the QS was deployed in section 121 on 99 level 44 x/c East 5 panel. Data from this site are not available due to a disc crash.

Seismic event with magnitude 2.9 It was expected that this event should cause extensive damage. A group of rock engineers from Mponeng mine visited the site immediately after the event. There was no extensive damage observed but there were indications of recent ground shaking in the face area. The mine network estimates seismic source parameters using far field data. A magnitude is estimated from seismic moment (low frequency radiation) and seismic energy. Fortunately, those two seismic source parameters are modelled independently, therefore they informed us - in an objective way - that the event was of large size or large deformation (seismic moment log Mo = 13. 2 [log Nm]) and associated with radiation with a large amount of seismic energy (log E = 8.2 [log J]). Therefore, one could expect that an event occurring close to an active stope should cause damage.

We will try to explain why this event did not cause damage.

The event was located some 100 m from the strong ground motion instrument, in the

hangingwall, 30 m above the QS. The first aftershock was recorded 0.4 s after the main event and the second aftershock 0.2 s later. The ground motion recorded in the hangingwall was to only a small degree affected by the medium, therefore directly revealing a history of the rupture process of the seismic source. The duration of strong ground motion caused by the S-wave group of the main event was 0.2 s. The S-wave group started with a small pulse with peak ground acceleration reaching 12 m/s^2. The second pulse arrived after 0.05 s and it was the strongest ground motion with a peak ground acceleration of 110 m/s^2 and duration less than 0.02s. The next interval of ground motion had an amplitude similar to the first pulse but the frequency was much lower and the duration longer. This interval could be a composition of one or two pulses.

The strongest peak ground acceleration is associated with the second pulse but its duration is only 0.02s (50Hz) so this is not a large event. Assuming that the rupture velocity is 3000m/s, the dimension of the sub-event is about 60m. The third group of ground motion could be associated with a larger subevent (low frequency) but much slower (small acceleration amplitude 50 m/s^2).

In summary, the seismic energy of this event was released in a series of subevents, each subevent had different seismic properties, but none of them was able to cause damage. However, following the popular Brune's model, this seismic event was understood as a uniform rupture process (one pulse) with rupture time less than 0.1 s and source size less than 200m. An analysis of the waveform shows that Brune's model does not approximate the observed event.

The above example shows that the rupture time of a seismic event should be used as an additional parameter to estimate the damage caused by the event. Fortunately, information about rupture time is available in far field data. Detailed analysis of the source time function was conducted using data from the mine network. The exact properties of subevents do not relate to the near field observation, the QS data, but the rupture time in both cases is the same.

3. Examination of support motion caused by seismic load.

An experiment was conducted to monitor the motion of support under a seismic load. The support units have been exposed to two major forces. One load is applied from the hangingwall and another from the footwall. Observations show that amplitudes of the applied accelerations or velocities from the hangingwall and footwall are not equal. Figures in Appendix 1. show examples of the motion of the support at three points and the ground motion at the surface of the hangingwall and footwall. Seismograms displayed in Figures A1 to A26 are near-field strong ground motions with large values of peak ground accelerations (PGA) and peak ground velocity (PGV). For the clarity of presentation, only a few examples are shown in this chapter. The rest of the examples are shown in Appendix 1. The figures show ground acceleration and velocity.

The velocity and the displacement are calculated by integration of ground acceleration. The velocity of ground motion is obtained by the integration of an accelerogram and in the same way displacement ground motion is resolved from velocity ground motion. Integration is performed using the widely recommended method of Newmark. Integration of seismic records is a very unstable task due to the presence of noise in the signal. The process of integration cumulates low-frequency noise present in the accelerograms. It is not difficult to remove this characteristic effect using high pass filters, but usually corrections deform the shape of the original signal. Therefore, it is better to use a short time series to reduce the negative effect of integration or a long time series before the arrival of a seismic event and subtract the polynomial that is responsible for destroying the zero level line. Several tests with different parameters of the integration routine allow a confidence to be developed in the calculation of the velocity of ground motion, values of peak ground velocity (PGV), peak ground displacement (PGD) and other major features of waveforms.

Figure 3.1 shows the five accelerograms of the seismic event of 1.1 magnitude. The QS site was situated less than 65 m from the seismic source. The five sensors were installed at the surface of the hangingwall, in the top of the support, in the middle of the support, in the bottom of the support and at the surface of the footwall. Figure 3.2 shows the velocity of the ground and support motion for the same event. The applied seismic load occurred as a series of two impulses. All accelerograms and velocity records have a strong similarity. Accelerograms of the strong ground motion at the hangingwall and footwall manifest a strong similarity, the major phases can be identified on both records. The velocity of the ground motion has more common features than the accelerograms. It is clear that the strong ground motion from the hangingwall is passed to the first accelerometers in the pack, almost without significant distortion. The same pattern of resemblance is observed between waveforms recorded at the footwall and in the bottom of the support. The support motion in the middle point could be modeled as the average value of the hangingwall and footwall motion.

When the source is located above the stope the strongest ground motion is at the surface of the hangingwall, as is expected. The amplitude of the signals gradually decays from the hangingwall towards the footwall; this is caused by attenuation of the seismic waves.

The ground motion presented in the Figures 3.3 is not very strong, it is caused by a seismic event of magnitude 0.8 located at a distance of less than 50 m from the sensors. A detailed analysis revealed several important features of the support motion. The support was struck with a load from the top (hangingwall) with a signal of low frequency. The velocity waveform reveals the nature of that load. As the signal is gradually attenuated (see Figure 3.4) most of the shape of the waveform is preserved in all five records starting from the hangingwall, through the three positions in the support and into the footwall.

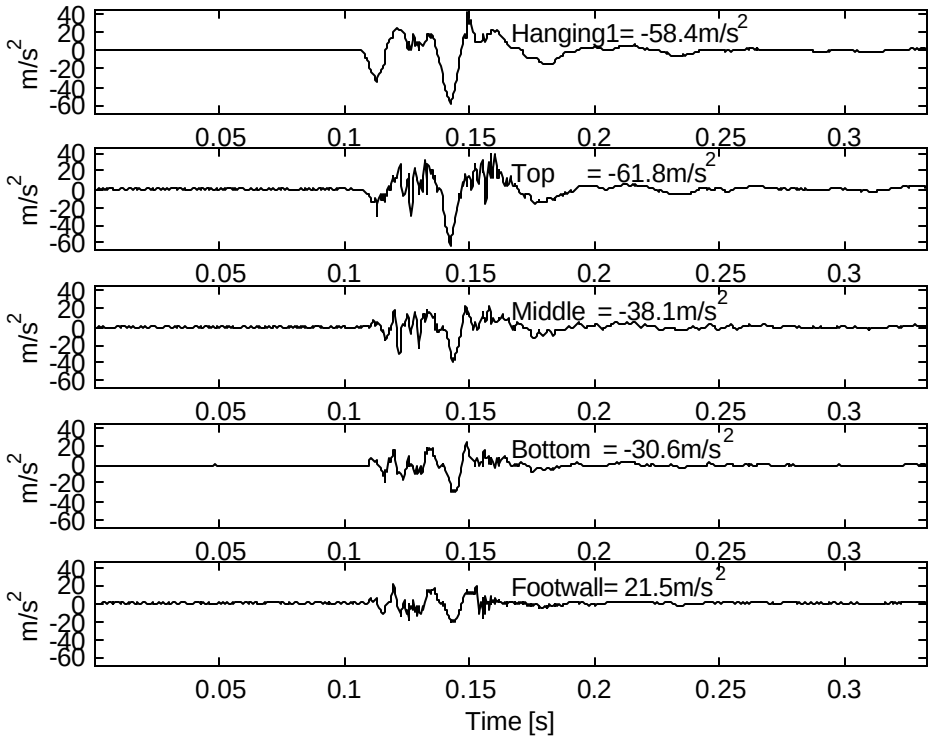

Figure 3.1 Seismic event with magnitude 1.1 located above the stope, less than 65 m from the strong ground motion sensors, Mponeng Mine 6 January 2002, 00:24hr. The five sensors were installed at the surface of the hangingwall, in the top of the support, in the middle of the support, in the bottom of the support and at the surface of the footwall

.

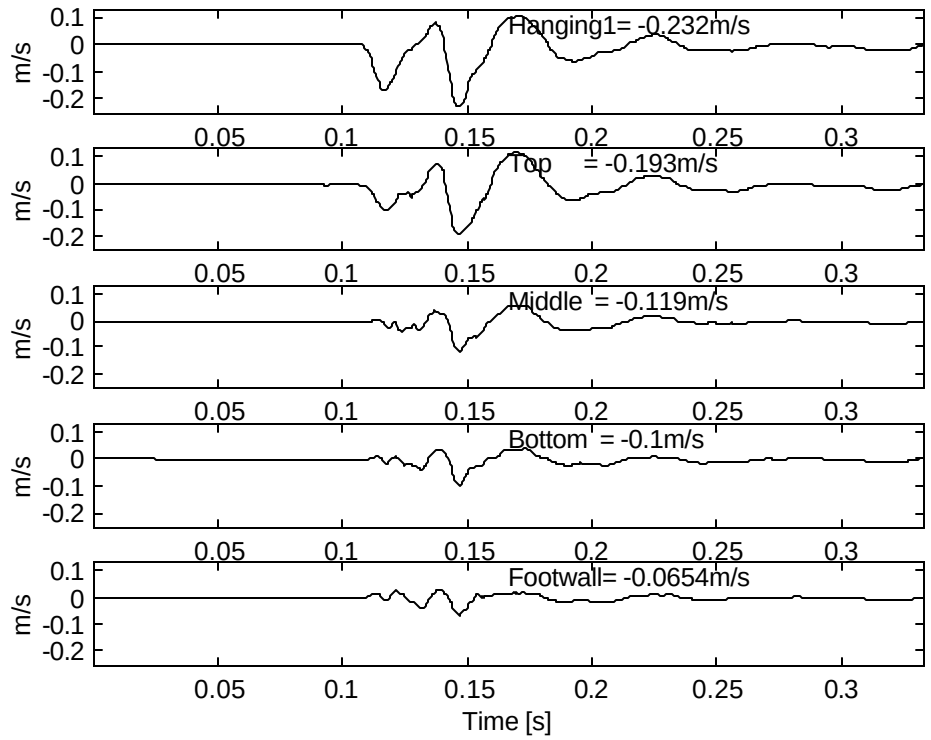

Figure 3.2 The velocity of ground and support motion calculated from accelerograms presented in Figure 3.1.

Figures 3.3 show the high frequency impulse, which originated in the footwall at time 0.1 s. This strong impulse is propagated from the bottom to the hangingwall. This impulse has a frequency content higher than 200Hz . The impulse was removed from the seismogram by the application of a band pass Butterworth filter with the lower cut-off 6Hz and the high cut-off 200Hz (see Figure 3.4). The nature of that impulse is not clear. It is not a small seismic event located below the stope, as a similar feature is observed during other events (see Figure 3.1 and Appendix 1) . This impulse has not originated in the support, because the strongest amplitude is observed in the footwall. All the above implies that it must, therefore, be some feature of the stope response.

The detailed inspection of the accelerograms reveals an additional complication in the support motion. Figure 3.6 (top) shows the overlaying motion recorded at the surface of the hangingwall and the footwall. The amplitude of hangingwall motion is larger than that at the surface of the footwall. The waveforms have synchronized phases, almost for the entire duration of motion, except for the initial interval of 0.025 s. The first pulse down and second swing up in the hangingwall correspond to a small impulse in the footwall, of which the polarity is shifted 180 degrees. The motion at the surface of the hangingwall and footwall determine the motion of the support. Figure 3.6 (bottom) shows the five overlaying accelerograms from Figure 3.1. An initial part of the motion in the top point of the support follows closely the motion of the hangingwall. The same

relationship is observed between the motion of the bottom of the support and the footwall. These motions are in phase. The interesting phenomena occur in the support between the top point and the middle point, because the support has to accommodate two loading forces acting in opposite directions. The differences between the rest of the five accelerograms could be described by the attenuation mechanism, as waves are progressing from the top point to the bottom point.

Data (see Appendix 1) show several examples where inputs from the bottom and top have similar amplitude and frequency content. Those examples had top support motion very similar to the hangingwall and the bottom support motion very similar to the footwall ground motion. The motion of the middle of the support shows a lack of similarity to the motion above or below; the motion of the middle point is a composition of both motions.

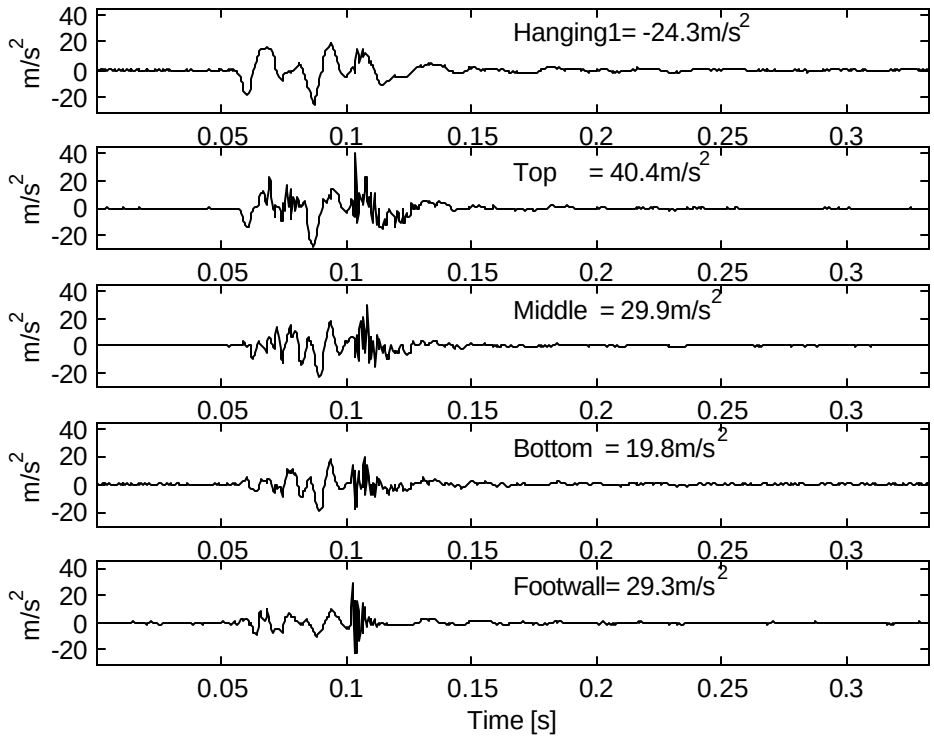

Figure 3.3 A seismic event with magnitude 0.8 located above the stope, less than 50 m from the strong ground motion sensors, Mponeng Mine 13 January 2002, 11:51hr. The five sensors were installed at the surface of the hangingwall, in the top of the support, in the middle of the support, in the bottom of the support and at the surface of the footwall. Note the high frequency impulse in the footwall record (around 0.1 s) This impulse propagates throughout the support.

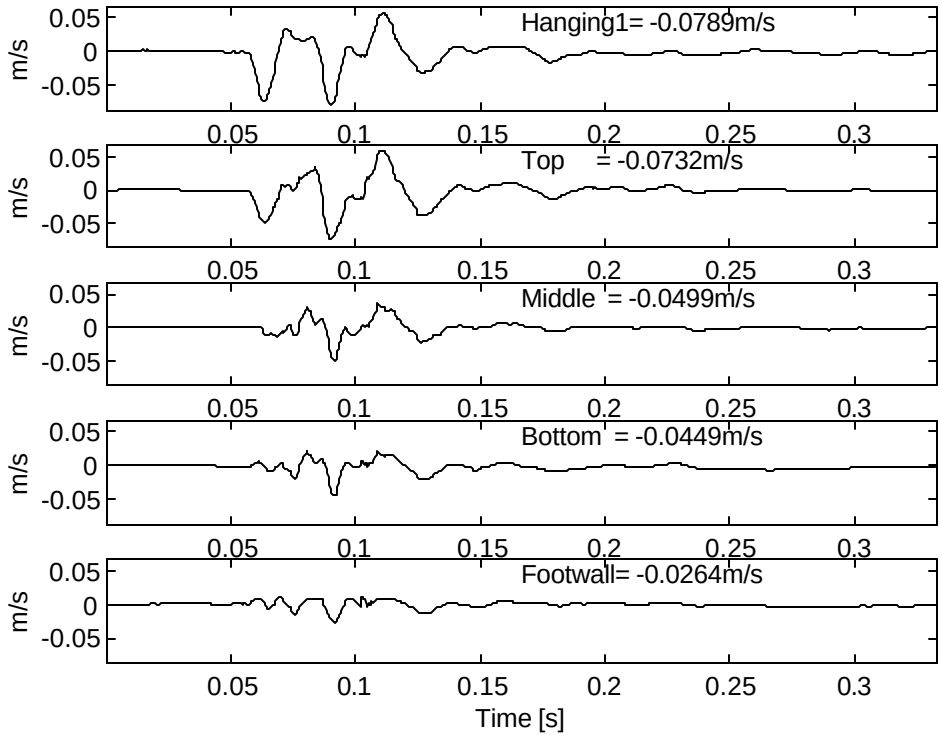

Figure 3.4 The velocity of ground and support motion calculated from accelerograms presented in Figure 3.3

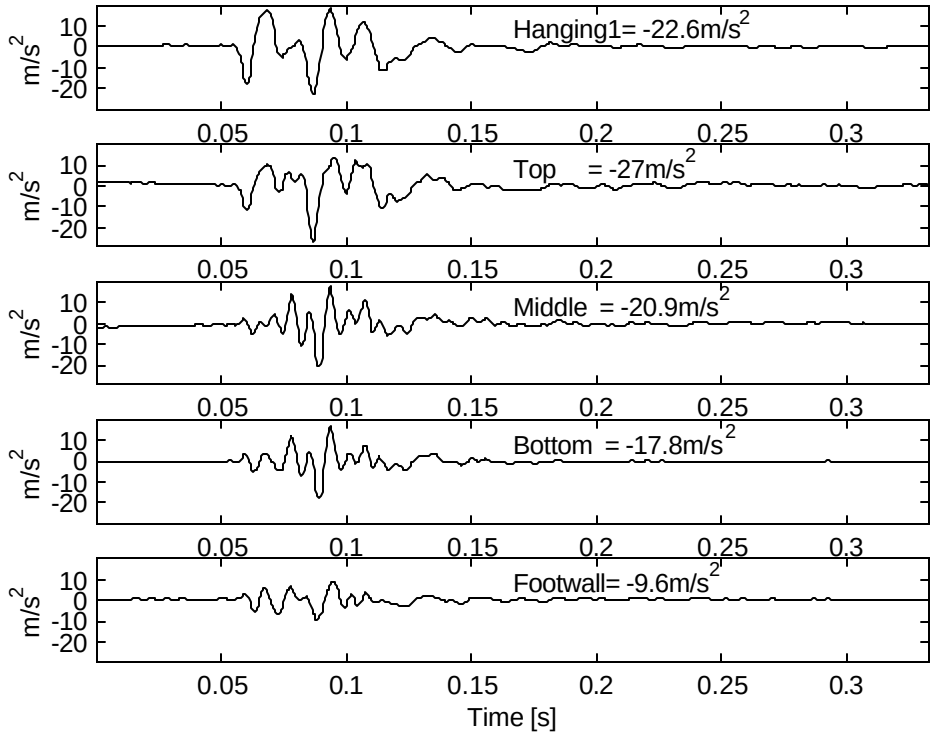

Figure 3.5 The filtered accelerograms of the event from Figure 3.3. The band pass Butterworth filter was applied with the pass band 6Hz - 200Hz. The high frequency impulse is removed from the seismograms.

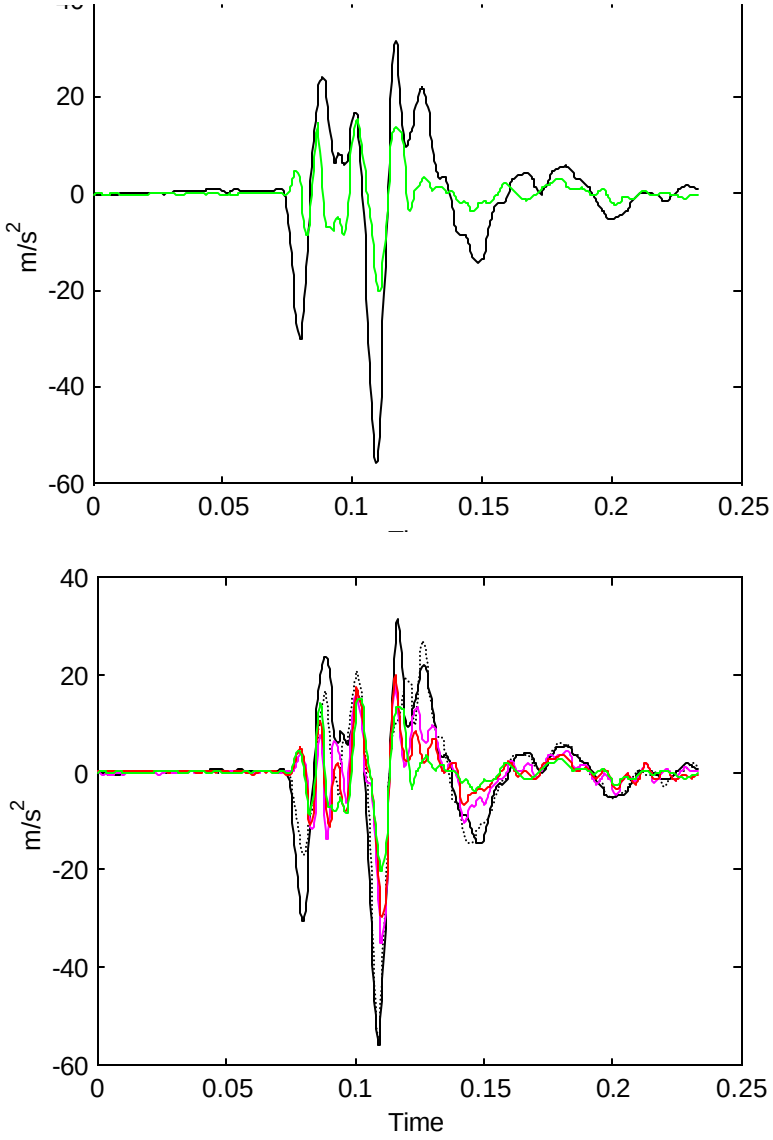

Figure 3.6 (top) Two overlaying accelerograms recorded at the surface of the hangingwall and the footwall respectively and (bottom) five overlaying accelerograms from Figure 3.1 The majority of the waveforms have a synchronised phase with the exception of the first impulse of the hangingwall and top support

The strongest recorded ground motion was caused by a seismic event of magnitude 1.8 located less than 40 m from the QS site and above the stope (see Figure 3.7). The inspection of the waveform shows the amplification of the high frequency component of the motion of the support. The effect of amplification is especially evident in the top point of the support.

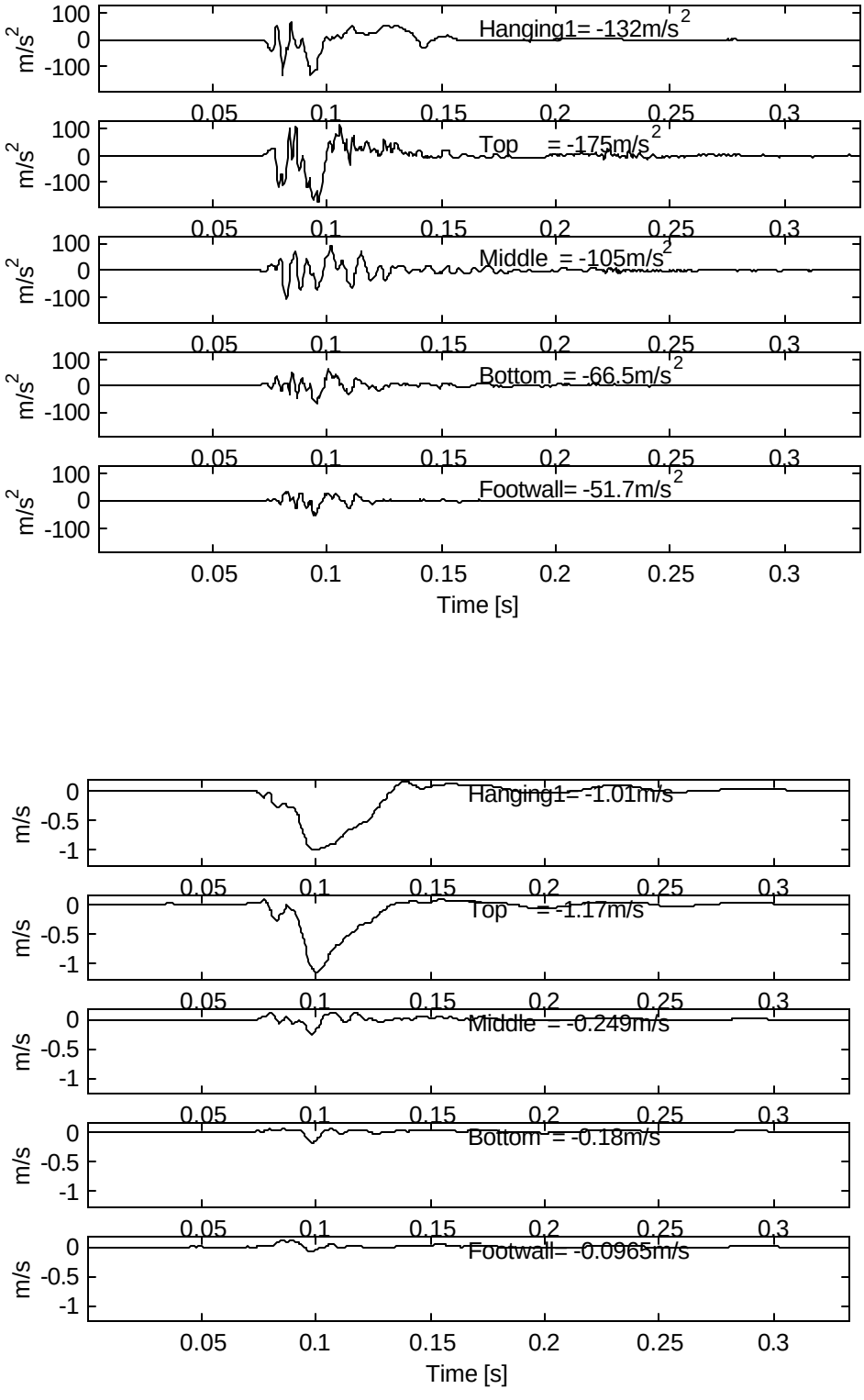

Figure 3.7 Acceleration (top) and velocity (bottom) of the seismic event with magnitude 1.8 located above the stope, less than 40 m from the strong ground motion sensors, November 22 2001, 21:12hr

The sensor installed in the support shows a significant reduction in the low frequency content in comparison to the sensor installed in the hangingwall. This effect is - to some extent - unsuspected. The small dimensions of the support could not be responsible for attenuation of a wave with a wavelength of 140 m
(V_s . Dominant period =3600m/s . 0.04s). The phenomenon could be explained using the dimensions of the stope. The event happened above the stope. The waves radiated from the seismic source at some stage reached the hangingwall layer (see hangingwall seismogram Figure 3.7). Next they passed through the stope layer (see three points of support motion Figure 3.7) and later propagated through the footwall layer(see the footwall seismogram Figure 3.7). The stope layer is composed of a few hundred packs and backfill. It is not a good medium for transmission of the seismic energy, therefore a strong attenuation is observed. The physical properties of a single pack have no influence on the process of attenuation of the low frequency signal. The difference in ground motion in the hangingwall and footwall has an effect on the way the pack is deformed. At this stage one thing is clear - a pack is not moving as one uniform block. The relative movement of the hangingwall with respect to the footwall determines the deformation of the pack.

The last group of examples has a motion which is amplified inside of the support, and inputs from the hangingwall and footwall are weaker than the observed amplitude in the support. Figure 3.8 and Figure 3.9 show the effect of this amplification of the velocity in the support in comparison to the input acceleration in the hangingwall and the footwall. The pattern of support motion caused by high frequency ground motion is not as clear as it is for strong ground motion. Therefore parameters of weak ground motion cannot be used as an indicator of the support's behavior under strong ground motion. The weak ground motion reveals a total lack of coherence between ground motions in the hangingwall and footwall, i.e. the major impulses are not in phase at all. In most cases, ground motions at the hangingwall and footwall are not alike. The records of weak ground motion dominate the available databases of in-stope ground motion measurements. Such data is mostly useless, as it does not carry information about damaging ground motion. Collected records reveal that the support response to strong ground motion is essentially different to the support response to weak ground motion (see GAP709b).

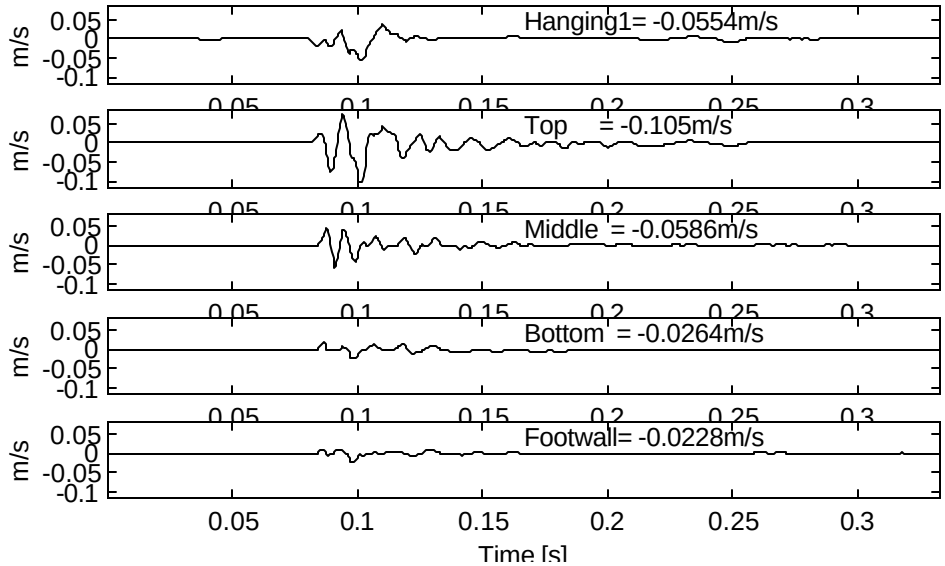

Figure 3.8. A seismic event with magnitude 0.4 located 150m from the strong ground motion sensors, November 22, 2001, 21:01hr. The event is located below the stope.

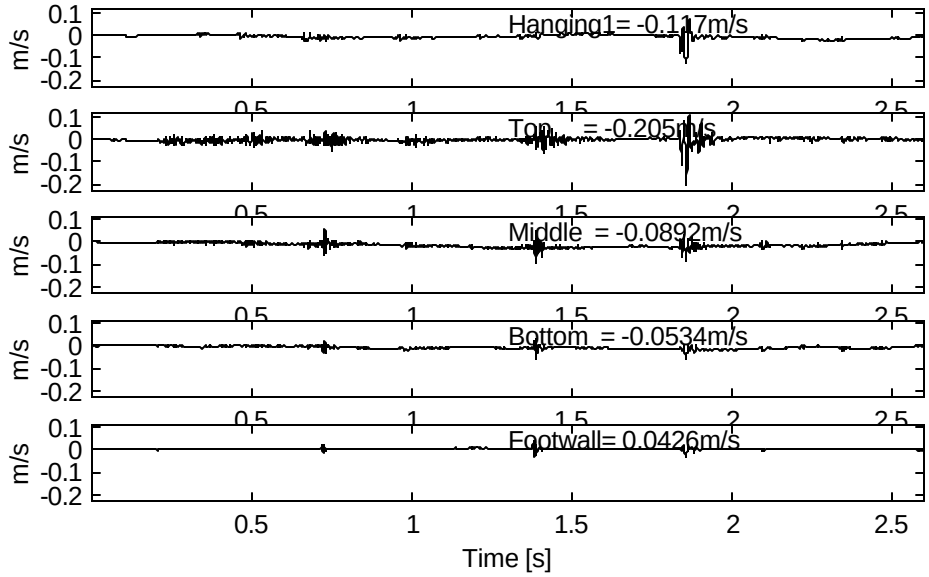

Figure 3.9. A series of seismic events, November 21, 2001, 18:23hr. Note the amplification of the signal in the support.

The terms "strong ground motion" and "weak ground motion" are used to classify the observed records. In this report strong ground motion is used to describe seismograms characterised by few oscillations and a dominant pulse with a strong component of low frequency. The spectrum of strong ground motion is usually broad band, so a high frequency signal is present as well (see GAP709b). Seismograms described in this way are the near-field records, where the distance between seismic source and the sensors is small. Weak ground motions have, by definition, smaller signal amplitude than strong ground motion. For small seismic sources the weak ground motions have a strong component of high frequency, however, for large seismic events located far from the sensor, weak ground motion is reached at low frequency.

A timber pack is deformed non-uniformly in its volume. The deformation of support between the five observation points is given by the following set of differences:

$$\begin{aligned} &u_h(t) - u_t(t) \\ &u_t(t) - u_m(t) \\ &u_m(t) - u_b(t) \\ &u_b(t) - u_f(t) \end{aligned} \qquad 3.1$$

For example, the deformation between the hangingwall and the first 25 cm of support is given by the difference $u_h(t) - u_t(t)$, the deformation between the top point of the support and the middle point of the support is given by $u_t(t) - u_m(t)$. The support has to accommodate the entire difference in displacement between the hangingwall and the footwall, $u_h(t)-u_f(t)$. The strongest ground motion recorded during the experiment is used to display the influence of the different layers of support on the seismic signal. Figure 3.10a shows the difference in acceleration between sensors. Figure 3. 10.b and Figure 3.10c represent the estimates of the relative velocity and displacement. The compressed information about ground motion parameters for the event of 1.8 magnitude is shown in Table3.1. The differential peak ground displacement, PGD, peak ground velocity, PGV and peak ground acceleration, PGA are displayed for each layer of the support. The velocity difference is proportional to the damping force, the displacement difference is proportional to the deforming force in the layers of the support. The largest deformation and attenuation occurred between the top and the middle points of the support. The deformation is not uniformly distributed across the support.

Table 3.1

Differences of the ground motion parameters in the layers of the support
for the event of magnitude 1.8 less than 40m distant from the array of sensors

Differences:	PGD [mm]	PGV [m/s]	PGA [m/s^2]
Hangingwall-Top	6.4	0.25	148
Top – Middle	23.6	1.16	187
Middle - Bottom	0.9	0.13	116
Bottom- Footwall	1.2	0.09	39
Hangingwall -Footwall	31.4	1.01	161

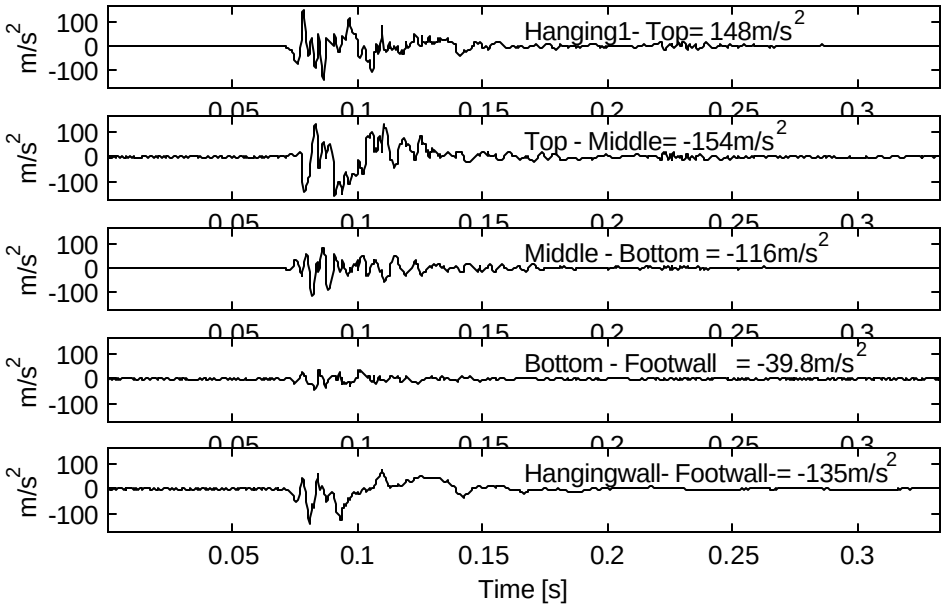

Figure 3.10a The differences in acceleration between the layers of the support. The strong ground motion is caused by a seismic event with magnitude 1.8 located above the stope, less than 40 m from the strong ground motion sensors, November 22 2001, 21:12hr.

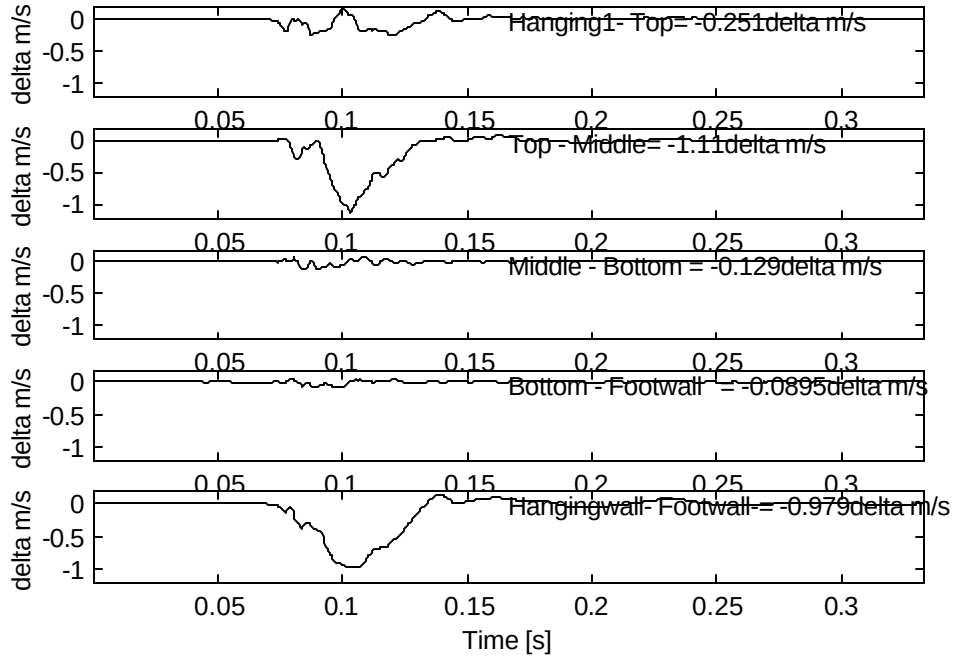

Figure 3.10b Estimates of the velocity differences between the layers of the support

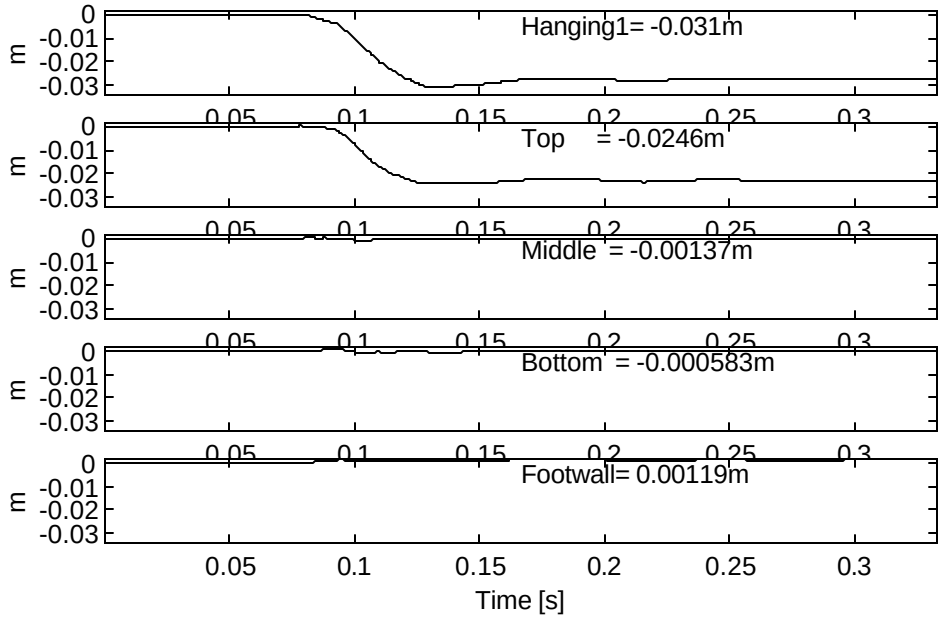

Figure 3.10c Estimates of the displacement differences between the layers of the support.

Summary of qualitative analysis

Strong ground motion:

1 The support motion at the top point follows the shape of the strong ground motion at the surface of the hangingwall, the same pattern of similarity is observed between the bottom point of the support and the footwall.

2 A seismic signal is strongly attenuated as it passes through the support. Closer inspection reveals that the amplitude of the motion at the top point of the support is very often stronger than the input signal from the hangingwall.

3 The same timber pack could be deformed uniformly and very non-uniformly in its volume. The differences in pack response are observed even in cases when signals are radiated from the same direction. Data shows that the strong nonlinearity of the support response is controlled by the amplitude of the strong ground motion.

Weak ground motion:

A seismic signal is strongly amplified in the support. The effect of amplification starts at the bottom or the top point of the support and, subsequently, the signal is attenuated as it progresses throughout the support.

4 Models of support response to seismic (cyclic) load

4.1 Multi-degree -of -freedom models of support response

In its most fundamental form, the seismic response of the structure, whether linear or nonlinear, is a solution of equations of motion. The model of linear elastic response of the structure has been almost universally used to model strong ground motions. Considering all of the observations of attenuation within the support pack, as described above, a damping force is included in the equation of motion. In this study, the equations of motion are solved for a vertically propagating wave by approximating the support as a stack of masses interconnected by springs. In such an idealization the mass of the structure is considered to be concentrated at a certain finite number of mass points and the resistance of the structure to deformation is then represented by structural stiffness and damping. In the elastic range the resistance is given by $f_s = k*\Delta u$, the spring stiffness, k, relates to the support layer's stiffness. The resistance damping force, f_d, relates to the viscous damping coefficient, c, by $f_d = c\,\Delta v$ where v is the velocity (the time derivative of u).

In this one-dimensional equation, only one vertical component of displacement is used. The differential equation of motion for each mass, m_i, can be written as

$$m_i\,\ddot{u}_i - c_i(\dot{u}_{i-1} - \dot{u}_i) + c_{i+1}\,(\dot{u}_i - \dot{u}_{i+1}) - k_i\,(u_{i-1} - u_i) + k_{i+1}\,(u_i - u_{i+1}) \;=\; 0 \qquad 4.1$$

where c_i, k_i and u_i are the damping coefficient, spring stiffness and absolute displacement respectively associated with the ith mass and a super dot (.) represents the time derivative. Similar equations for the motion of all the masses can be written except for the boundary conditions of the system at the first, i=1, and the last spring, i=N. The support has the boundary condition fixed at both ends. The general idea is that the load is applied from both directions: i=1 and i = N then u_o is the displacement imposed by the hangingwall and u_N is the displacement imposed by the footwall. If a load is applied only from one direction for example from i= 1, then $u_{i+1} = 0$. In the undesirable case when support does not touch the hangingwall at the top, a spring has $k_o = 0$. It is the free boundary condition.

The process by which vibration steadily diminishes in amplitude, is called damping. The energy of the vibration system is dissipated by various mechanisms. Most of the energy dissipation arises from the thermal effect of repeated elastic straining of the material and from the internal friction when a solid is deformed by opening and closing of micro cracks in concrete. It seems impossible to identify or describe mathematically the dissipating mechanisms of this energy in an actual structure. As a result, the damping in an actual structure is represented in an idealized manner. For many purposes, the actual damping in a single-degree-of-freedom (SDOF) system, is idealized satisfactorily by a linear viscous damper. The damping coefficient represents all possible damping mechanisms. The viscous damper is intended to model the energy dissipation at deformation amplitudes within the elastic limit of the overall structure. The vibration experiments on an actual structure provide the data for evaluation of the damping coefficient.

How many degrees of freedom have to be used to model a support motion? This problem will be discussed in great detail. The mass of an actual structure is continuously distributed over the spatial extent of the structure, and, as a result, actual structures have an infinite number of degrees of freedom as far as vibration is concerned. Often however, the important features of the dynamic response of an actual structure may be adequately approximated by idealizing the structure. A support is represented by an idealized system with rigid masses, springs and viscosity, where the masses are assumed to be constrained to move only in a vertical direction. The support unit may be considered as a dynamic system with SDOF, if one number is required to define the displacement of all the masses of the support unit relative to their original position. However, if the different sections of the support unit have different displacements, a multi-degree-of-freedom (MDOF) model has to be used. The general theory for evaluating the dynamic response of a concentrated mass system with multiple degree of freedom was developed by Clough and Penzien, 1975.

An inspection of the data indicated that the three points of the support have different motion. The first choice of model for the support is the one which could utilize all the data. Figure 4.1 shows a 3 degree-of freedom (3-DOF) structure, which is an example of MDOF systems. The support is represented by arrangements of concentrated masses

supported or connected by springs and dampers. Newton's second law for each mass is given by the following equations:

$$\begin{aligned} m_1 \ddot{u}_1 &= f_2 - f_1 \\ m_2 \ddot{u}_2 &= f_3 - f_2 \\ m_3 \ddot{u}_3 &= f_4 - f_3 \end{aligned} \qquad 4.2$$

and related restoring forces are

$$\begin{aligned} f_1 &= k_1 (u_1 - u_0) + c_1 (\dot{u}_1 - \dot{u}_0) \\ f_2 &= k_2 (u_2 - u_1) + c_2 (\dot{u}_2 - \dot{u}_1) \\ f_3 &= k_3 (u_3 - u_2) + c_3 (\dot{u}_3 - \dot{u}_2) \\ f_4 &= k_4 (u_4 - u_3) + c_4 (\dot{u}_4 - \dot{u}_3) \end{aligned} \qquad 4.3$$

where u_1, u_2, u_3 are the absolute displacements (total displacement)of mass m_1,m_2 and m_3 respectively and u_0 ,u_4 are the displacements at the surface of the hangingwall and the footwall. The support is fixed at its ends. It should be noted that u_0 and u_4 are the displacements caused by fixed boundaries.

The stope support is exposed to footwall and hangingwall external loading which is applied simultaneously. The experimental measurements of loading and the acceleration of the support are available from a measurement.

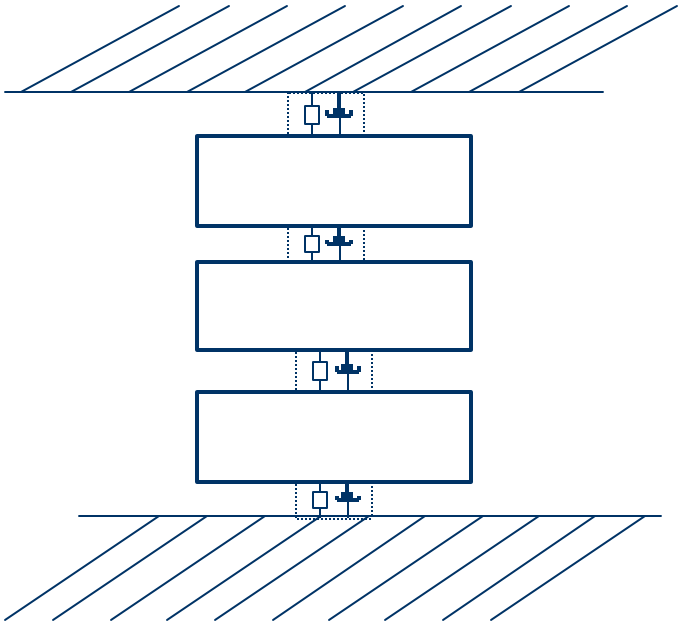

Figure 4.1 Support model - a 3-degree-of-freedom system subjected to the hangingwall u_0 and the footwall u_4 motion.

Combine and simplify the equations

$$\begin{aligned} m_1\ddot{u}_1 + (k_1 + k_2)\,u_1 - k_2u_2 - k_2u_o + (c_1 + c_2)\,\dot{u}_1 - c_2\dot{u}_2 - c_2\dot{u}_o = 0 \\ m_2\ddot{u}_2 + (k_2 + k_3)\,u_2 - k_3u_3 - k_2u_1 + (c_2 + c_3)\,\dot{u}_2 - c_3\dot{u}_3 - c_2\dot{u}_1 = 0 \\ m_3\ddot{u}_3 + (k_3 + k_4)\,u_3 - k_4u_4 - k_3u_2 + (c_3 + c_4)\,\dot{u}_3 - c_4\dot{u}_4 - c_3\dot{u}_2 = 0 \end{aligned} \qquad 4.4$$

The second model of support has two masses, three springs and dampers. The model is motivated by observations described in chapter 3. A significantly different load is applied to the support pack from the direction of the hangingwall and the footwall. Due to asymmetry of the loads there is a possibility that damage to the support will be observed only from a side where the strongest load has been applied. Figure 4.2 shows the 2 -degree of -freedom support model. The equations of motion is given by

$$\begin{aligned} m_1\ddot{u} &= f_2 - f_1 \\ m_2\ddot{u}_2 &= f_3 - f_2 \end{aligned} \qquad 4.5$$

Where

$$\begin{aligned} f_1 &= k_1(u_1 - u_0) + c_1(\dot{u}_1 - \dot{u}_0) \\ f_2 &= k_2(u_2 - u_1) + c_2(\dot{u}_2 - \dot{u}_1) \\ f_3 &= k_3(u_3 - u_2) + c_3(\dot{u}_3 - \dot{u}_2) \end{aligned} \qquad 4.6$$

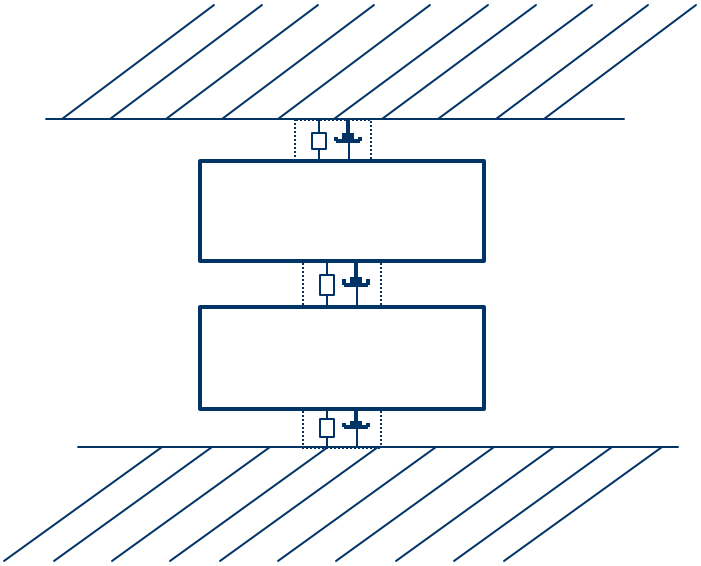

Figure 4.2 Support model - a 2-degree-of-freedom system subjected to the hangingwall u_1 and the footwall u_0 motion

The equations of motion after substitution in equation 4.6 become

$$m_1\ddot{u}_1 + k_1(u_1 - u_0) - k_2(u_2 - u_1) + c_1(\dot{u}_1 - \dot{u}_0) - c_2(\dot{u}_2 - \dot{u}_1) = 0$$
$$m_2\ddot{u}_2 + k_2(u_2 - u_1) - k_3(u_3 - u_2) + c_2(\dot{u}_2 - \dot{u}_1) - c_3(\dot{u}_3 - \dot{u}_2) = 0 \qquad 4.7$$

Assuming that $k_1=k_2=k_3=k$, $c_1=c_2=c_3=c$ and $m_1=m_2=m$ equation 4.7 leads to

$$m\ddot{u}_1 + k(2u_1 - u_2\ u_0) + c(2\dot{u}_1 - \dot{u}_2 - \dot{u}_0) = 0 \qquad 4.8$$
$$m\ddot{u}_2 + k(2u_2 - u_3\ u_1) + c(2\dot{u}_2 - \dot{u}_3 - \dot{u}_1) = 0$$

Equation 4.8 expresses the support motion using the absolute displacement, u_0 and u_3. To gain some insight into the process of deformation of the structure, the absolute (total) displacement has to be decomposed into a sum of the displacements due to stope motion, u_s, and the dynamic displacement, u_r, of the support. The u_r represents the relative displacement between the mass and the ground. At each instant of time these displacements are related by

$$u_1 = u_{r1} + u_{s1} \qquad 4.9$$
$$u_2 = u_{r2} + u_{s2}$$

where u_{s1} , u_{s2} are given by the following expressions (see Newmark, and Rosenblueth, 1971 Chapter 2)

$$u_{s1} = (2u_o + u_3)/3 \qquad 4.10$$
$$u_{s2} = (2u_3 + u_0)/3$$

Solving the MDOF problem involves determination of the frequencies and shapes of the normal modes of vibration of the system. The dynamic response of the system to a given dynamic load is then evaluated by superimposing the proper contributions of the various normal modes of vibration. The modal superposition method is especially applicable to the majority of structures that are designed to remain essentially elastic when subjected to medium intensity ground motions. The primary feature of modal analysis is that the total response of a structure is obtained by combining the response of its individual modes of vibration calculated separately. The result of this analysis is rather complicated and applies only to the particular type of structure analyzed. The model is not included in the scope of this project.

4. 2 Simplified mode of support response

It is possible to construct a model which can reproduce the structure's motion, but the extrapolation power of that type of model could be limited. The same complex model will not be suitable for a different unit of the same type of support. A simplified model, which can approximately measure the spatial effects of the support response, providing insight into the overall structural behavior under double loads is needed for applications. It is necessary to idealize both the structure and the loading. Engineering judgment and knowledge of the dynamics of structures are required to develop a satisfactory model that is both simple and representative of the most important dynamic behavior of the structure. The simplified model should approximately represent the significant features of the dynamic response of the support including the fundamental period and mode shape, as well as the effects of support-hangingwall and structure-footwall interaction. The features which are common for the several types of support should be well modeled. The natural frequency of the equivalent system must be the same as the actual structure. If the stope undergoes plastic deformation, the spring must also have plastic characteristics.

The simplified models have been developed for the timber pack. The simplified model rigorously accounted for the hangingwall-support-footwall interaction effects, as well as for the energy absorption of the support. Observations from the closely spaced strong ground motion array have shown that ground acceleration measured at different locations within the support is different. This effect is not handled by a SDOF system, therefore in the proposed model the deformations at the top and bottom points of the support do not have to be the same. It was assumed that support has a regular geometry and only vertical deformations are considered (one dimension problem).

Consider a single degree of freedom structure under double support loading. If one number or one coordinate can define the position of a structure, the structure is said to have one degree of freedom. The support can be represented by a single concentrated mass connected by springs with the hangingwall and the footwall (see Figure 4.3). It is assumed that due to seismic loading the support unit moves only in the vertical direction. When idealizing dynamic loads on the support, the simplifications required the geometric distribution of the load over the structure. If, for purposes of analysis, the mass of the system is concentrated at certain points, the load must be applied at the same points.

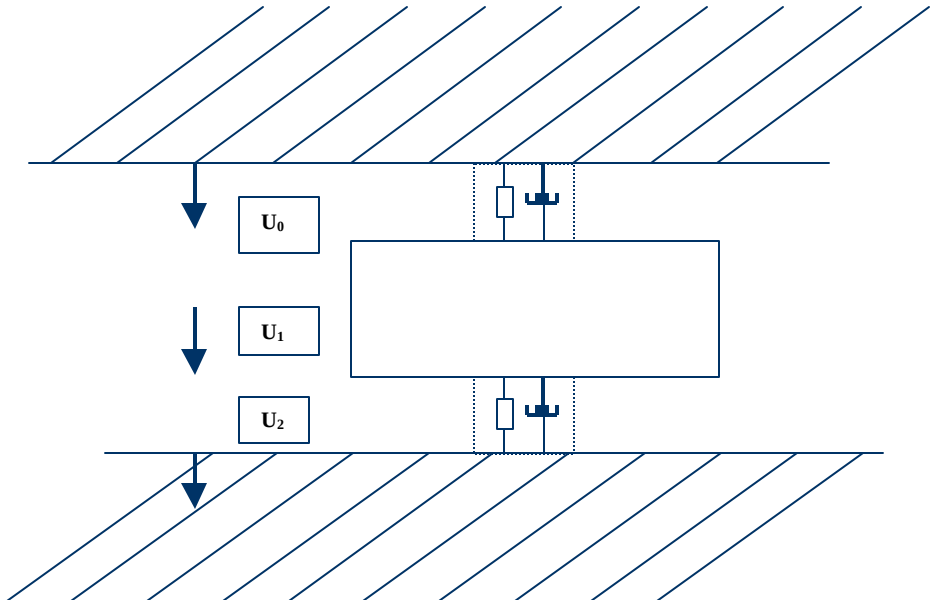

Figure 4.3 Support model - a one-degree-of-freedom system subjected to the hangingwall, $u_o = u_h$, and the footwall, $u_2 = u_f$ motion.

Figure 4.3 shows a SDOF support model. Under the action of the seismic event, u_f and u_h , the structure deforms and moves. The forces acting on the support along the vertical axis are the elastic or inelastic resisting force and the damping force. The equation of motion for a linear SDOF system may be written:

$$m\ddot{u} = f_2 - f_1 \qquad 4.11$$

where

$$f_1 = k_1(u_1 - u_0) + c_1(\dot{u}_1 - \dot{u}_0)$$

$$f_2 = k_2(u_2 - u_1) + c_2(\dot{u}_2 - \dot{u}_1) \qquad 4.12$$

The resulting equation of motion is

$$m\ddot{u}_1 - k_1(u_1 - u_0) + k_2(u_2 - u_1) - c_2(\dot{u}_1 - \dot{u}_0) + c_2(\dot{u}_2 - \dot{u}_1) = 0 \qquad 4.13$$

where $u_1(t)$ is the total (absolute) displacement of support, $u_o(t) = u_h(t)$ is the displacement of the hangingwall and $u_2(t) = u_f(t)$ is the displacement of the footwall. The $u_o(t)$ and $u_2(t)$ are the result of ground motion caused by the seismic event. The total displacement, $u_t(t) = u_1(t)$ of the mass may be expressed as its displacement due to application of the ground motion, $u_s(t)$, and dynamic displacement $u_r(t)$. In other words $u_r(t)$ is the relative displacement between the center of the support and the surfaces of the

stope, it is the deformation of the structure. The $u_s(t)$ is a quasi static displacement which represents the displacement of the support resulting from the static application of a ground displacement. In order to understand the interaction of a support with the hangingwall and the footwall the relative displacement, $u_r(t)$ should be used as an indicator of structure integrity, because the relative displacement is - in general- proportional to the strain inside a structure and the strain level is directly linked to structure damage.

Assuming that the pack has uniform properties in its volume, then $k_1 = k_2 = k/2$, where k is the stiffness of the support pack and $c_1 = c_2 = c/2$, where c is the viscous damping coefficient of the support pack. For this system, at each instance of time, a total displacement, u_t, is given by:

$$u_t = u_r + u_s = u_r + 1/2(u_f + u_h) \qquad 4.14$$

The relation $u_s(t) = ½(u_f(t) + u_h(t))$ is obtained by using the theory of multiple excitation (see Newmark, and Rosenblueth, 1971 Chapter 2 and Chopre 1995 Chapter 9.7) . The methodology was developed to formulate the equation of $u_s(t)$ when different motion is applied to different parts of the structure. The quasi-static displacement,$u_s(t)$, stands for the structural displacement referred to the static configuration imposed by the stope motion. The center of the support pack is not deformed when $u_r(t) = 0$ and $u_t(t) = u_s(t)$.

Substituting Eq. 4.14 into Eq. 4.13 leads to

$$m\ddot{u}_r + k\,u_r + c\,\dot{u}_r = -m(u_f + u_h)/2 \qquad 4.15$$

The term $-m(u_f(t) + u_h(t))/2$ is the effective force applied to the pack due to seismic excitation in the hangingwall and the footwall.

The SDOF model assumed that the support moves as a uniform block during a seismic event, therefore the restoring force, $f_s(t)$, should be characterized with one relative displacement. This is a limitation of the suggested support model. To overcome this predicament let's consider that the support is a column with a different load applied from the footwall and the hangingwall. The response force of the column at its end are given by the following formulae (Zembaty 1996):

$$f_h(t) = k/2(u_h(t) - u_1(t)) \qquad 4.16$$
$$f_f(t) = k/2(u_f(t) - u_1(t))$$

The equation 4.16 allows the analysis of the spatial seismic effect on the structure using the simplified model. Zembaty (1996) shows that the formula reflects the joint influence of the quasi-static and dynamic response of the structure.

4.3 Solution of equation of motion for inelastic deformation of support

A model of restoring force is needed to solve the equation of motion. The relationship between resisting force, $f_s(t) = k\, u_r(t)$, and deformation $u_r(t)$ used in section 4.2 is linear and elastic. The examination of the patterns of nonlinear stress -strain behavior for various materials under repeated and reversed load revealed hysteresis loops in the restoring force. (e.q Chopra 1995.) In general, the inelastic resisting force depends on the displacement and velocity of the deformations, $f_s(t) = f_s(u_r(t), v_r(t))$. There are many different nonlinear hysteresis models of the $f_s(t)$ that take into account a range of materials effects, such as strain hardening and degradation in strength or stiffness.

A manufacturer of support packs (e.q. Mondi) usually provides a load deformation curve for the monotonic loading obtained under a constant loading rate of 30mm/min. These data address the problem of stope closure. The stope closure and integrity of the strata dictate the primary support performance requirements. The nature of the seismic load is radically different than the nature of the load caused by stope closure. The load imposed by strong ground motion has a very high rate and has cycles. Figure 4.4 shows a schematic load deformation curve, where a support is exposed to long term deformation caused by the stope closure and seismic loads applied for short time.

The characteristics of the load deformation curve obtained under the monotonic load have limited use in evaluation of the attributes of the support under the seismic load. In these circumstances a model of response force has to be postulated. Typically an inelastic deformation is characterized by using an elasto-plastic and a bilinear model. For those models the shapes of hysteresis loops are schematically sketched on Figure 4.5. The load deformation function may be defined as a path dependent model (see Figure 4.5) with the following equation:

$$f(u_r, \dot{u}_r) = \begin{cases} \textit{if} \quad \dot{u}_r(t) > 0 & \\ \quad z_1 = A + k_1 u_r & \textit{where} \quad z_1 < z_2 \\ \quad z_2 = (k_1 - k_2)\, u_y + k_2\, u_r & \textit{where} \quad z_1 > z_2 \\ \textit{if} \quad \dot{u}_r(t) \le 0 & \\ \quad z_1 = A + k_1 u_r & \textit{where} \quad z_1 \ge z \\ \quad z_2 = -(k_1 - k_2)\, u_y + k_2\, u_r & \textit{where} \quad z_1 < z_2 \end{cases} \qquad 4.17$$

where A is the path dependent value. The load deformation is controlled by three parameters: yielding displacement u_y , yielding deformation, f_y and stiffness after linear deformation, k_2. The yielding displacement and force are used to calculate the initial elastic stiffness, k_1, of the support. The restoring force is a piecewise linear function of

displacement. The unloading stiffness is the same as the initial elastic stiffness. Figure 4.5 shows an example of the hysteresis loop for an inelastic response of the structure. Initially, the system is linearly elastic with stiffness k_1. When the system exceeds its yield deformation, u_y, its stiffness changes to k_2. The stiffness k_2 could be expressed as $k_2 = \alpha k_1$ where $\alpha > 0$. An elastoplastic system with $k_2=0$ is a special case of the bilinear model. The resisting force depends on the prior history of motion. Figure 4.5 shows a typical cycle of loading (A, B, C), unloading(C, D, E) and reloading (F, F,). Unloading from a point C takes place along a path parallel to the initial elastic deformation. The deformation increases during loading and reloading phases (velocity >0) and deformation decreases during the unloading phase (velocity < 0) . Note that negative deformation is permitted. Those three model parameters i.e. yielding force f_y, yielding displacement u_y and k_2 are sufficient to capture the essential features of the hysteretic behavior being modeled. An unloading branch is drawn parallel to the elastic branch of the bilinear or plasto-elastic skeleton.

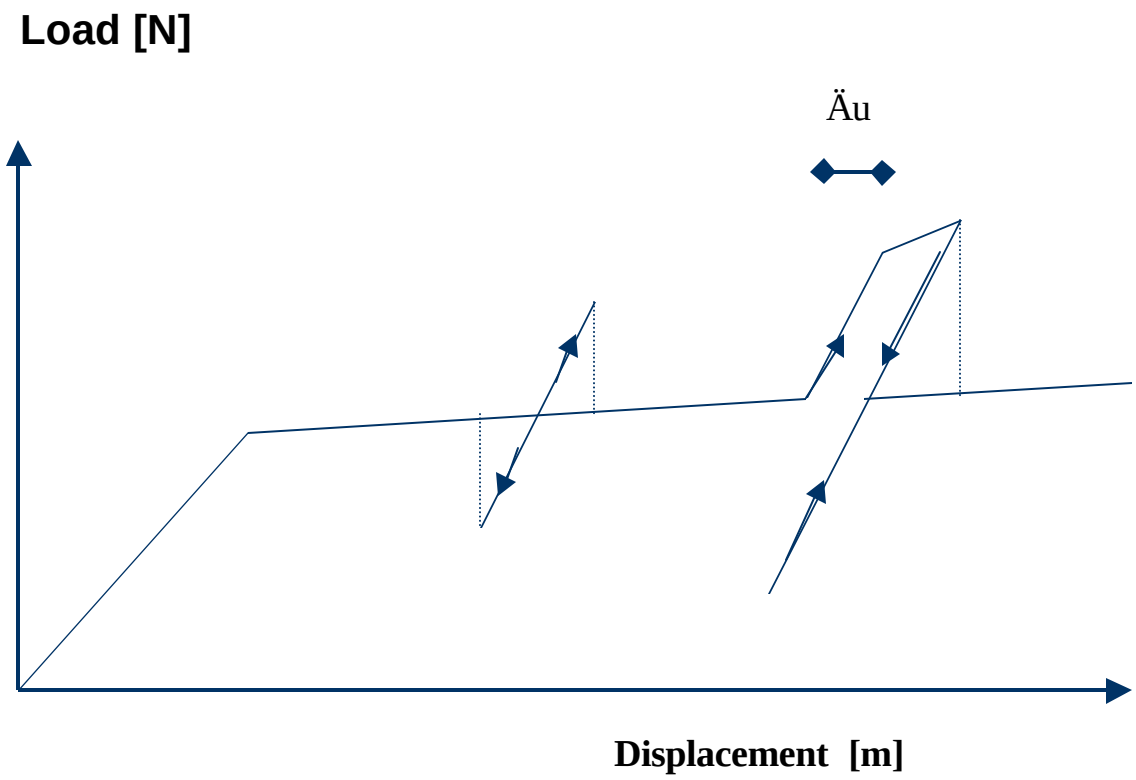

Figure 4.4 Schematic of deformation under load, where a support is exposed to deformation caused by the stope closure and seismic load. Two simple examples of seismic deformation are imposed on long term deformation. The first seismic event does not lead to permanent elastic deformation and the second event with stronger amplitude induced a permanent deformation, Δu . The two seismic loads are applied only for a short time

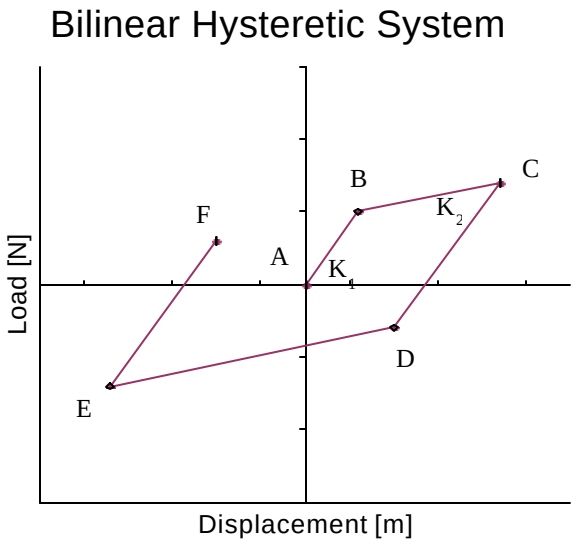

Figure. 4.5 The bilinear hysteretic load deformation model. $k_{1,}$ is the initial elastic stiffness, k_2 is the stiffness after yielding, u_y is the yielding displacement (displacement related to point B).

.

The energy input to a structure under seismic dynamic loading is dissipated as damping and inelastic deformation. The equation of motion for a single degree of freedom structure subjected to a seismic ground motion can be written as follows

$$m\ddot{u}_r + f_s(u_r \dot{u}_r) + c\dot{u}_r = -m(u_f + u_h)/2 \qquad 4.18$$

Numerical solution of the equation of motion Eq.4.18 with nonlinear deformation and real ground motion is needed. The differential equation is solved using the step by step linear average acceleration method (see Chopre 1995 Chapter 5). This method was selected because of its superior accuracy, although it is not as simple as the central difference method. Special attention was given to the precision of when the stiffness changes its values. The procedure with a constant time step could lead to unacceptable, inaccurate results. At the points where function f_s ($u_r(t)$, $v_r(t)$) switched to a different mode, an iterative procedure was used to calculate rapid variable stiffness in the model. The iteration was used to calculate an additional displacement to follow closely the nonlinear changes in the deformation force. A high precision of displacement calculations

is required at the points where load is reversed (velocity changes sign from positive to negative or from negative to positive). To solve equation 4.18 a computer program was developed in MATLAB. The waveform of ground motion recorded at a site in El Centro, California, during the Imperial Valley earthquake of May 18 1940 was used to check the software. This particular waveform is used as a standard in earthquake engineering.

The viscous damping coefficient, c, is often expressed as c = 2 â ù m where
â is the damping ratio or damping coefficient and ù is the natural frequency of the system.

4. 4 Data analysis

The objective is to calculate a theoretical response of the support using observed accelerograms recorded in the footwall and hangingwall. The load of the effective force on the support is defined by the right side of Eq. 4.15 or Eq 4.18.

$$m(u_h + u_f)/2$$

An adequate support model has to be able to predict the support motion caused by seismic load. The model of the structure is usually verified by comparing the observed motion with the theoretical one. The restoring force $f_s(u_r(t), v_r(t))$ acting on the support is controlled by three parameters u_y, f_y (or k_1) and k_2 and the actual shape of the hysteresis loop is controlled by the displacement and velocity of the support. The actual parameters of the restoring force are unknown. The estimation of those parameters may be obtained using time consuming 'try and guess' methods and the selection of parameters is later verified by matching the observed support response to the theoretical support response. A guideline to selecting an initial guess could be drawn from experiments with a slow monotonic load, because measurements in the laboratory indicate that the shape of the load deformation curve is similar for different loading rates.

In this experiment seismic data are collected for a timber pack (1.5x 1.5.1.3 mat pack) The estimated mass of a timber pack is 1000 kg (T. Coetzee of Mondi Mining Supplies). Mondi Mining Supplies provided the experimental load deformation curve obtained at the loading rate of 30mm/min= 0.005m/s. These experimental relationships and average distance from support to face were taken into account to estimate the load imposed by stope closure. The average load on a timber pack is 1200 kN (T. Coetzee of Mondi Mining Supplies, and T. Ward of Mponeng Mine). Timber is capable of being shaped by pressure in compression. The strength of timber under earthquake loads is substantially higher than for long term load, and an enhancement factor of 1.7 times the strength under slow load is used in the timber code (Dowrick D J, Earthquake Resistant Design). A similar relationship was developed by Taggart (GAP032) and used by Roberts (2000) to estimate the load deformation curves at a high rate of deformation. Neville Henderson of

Mondi Mining Supplies suggests that the maximal value of the enhancement factor is 1.5 for a composite pack. The relationship developed by Taggart is given by the following equation:

$$f_{fast} = f_{slow}\,(1.16)^{\log(v_{fast} / v_{slow})} \qquad 4.19$$

where f_{slow} is the peak load at lower velocity, f_{fast} is the peak load at high velocity, v_{slow} is the slow rate of load, v_{fast} is the fast rate of load. The above equation is used in the following way. The f_{slow} represents load caused by closure and equals 1200 kN for timber pack, v_{slow} = 0.005m/s. The v_{fast} is estimated from the average ground velocity of the group of S-waves and f_{fast} is interpreted as the yielding force of the dynamic load.

The yielding displacement, u_y, and the k_2 are estimated by comparing the observed motion of support with the theoretical one using only very strong ground motion records. The last parameter, which has to be estimated in an equation of motion, is a viscous damping coefficient, c. The damping force, which is controlled by the viscous damping coefficient influences only the later part of the theoretical seismogram and therefore is relatively easy to estimate.

It should be noticed that the slow static load imposed by the stope closure does not effect the dynamic structure response; in the equation of motion only a position of the central point is shifted. Therefore the value of the total force is calculated by adding the seismic load increment to the static support force.

Figure 4.6 shows a comparison between the observed velocity of the support center, $v_m(t)$ and velocity imposed by loading , $\frac{1}{2}(v_h(t) + v_f(t))$. The similarities indicate that the center of the support mostly follows the loading (see Figure 4.6 top). Figure 4.6 top shows the strongest difference between waveforms in the initial part of the record. The example from Figure 4.6 (bottom) displays the strong difference between waveforms, which indicates the large amplitude of the relative motion, $v_r(t)$. The differences between the observed velocity of the support center and velocity imposed by loading carry the information on the dynamic response of the center of the support, its duration, amplitude and frequency content.

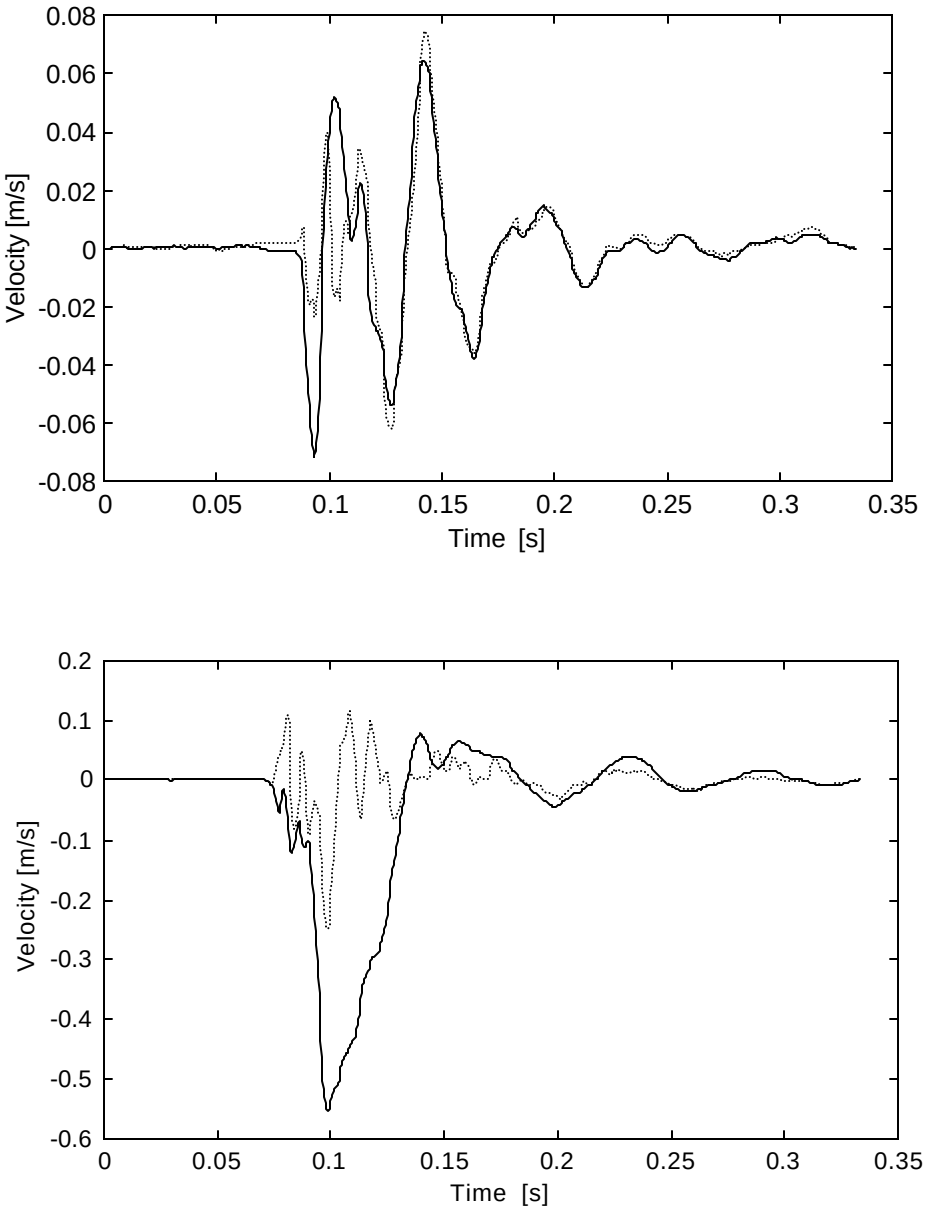

Figure 4.6 A comparison between the observed velocity motion of the middle of the support and the velocity of motion imposed by the loading (top). Magnitude 1.1, January 31 2002, 00:08:38hr (bottom). Seismic event with magnitude 1.8 November 22 2001, 21:12:03hr

First a ground motion with moderate amplitude and with a deformation in the elastic range was chosen for analysis. Its seismograms are used to estimate the stiffness, k1 of the structure. The calculation was made in frequency range from 5 Hz to 1300 Hz. A process of calculation of the theoretical response involves the integration of the waveform, therefore there is always a possibility of amplifying the low frequency noise. Repeating the experiment in a different frequency range controlled this effect. The lower cutoff frequency of 5 Hz or 10 Hz gives a reasonable fit to the acceleration and velocity waveforms. The theoretical waveforms of $v_m(t)$, $a_m(t)$, $v_r(t)$ and $a_r(t)$ were used to reproduce the major features of acceleration and velocity records from the data. The four theoretical curves were computed to get a reasonable estimation of the k_1 stiffness. The estimation is not easy, because the total motion of the middle of the support $v_m(t)$, $a_m(t)$ is dominated by the hangingwall and footwall motions. Another source of error could be introduced by $v_r(t)$, $a_r(t)$. The observed relative motion of the middle of the support is obtained by adding and subtracting the observed accelerograms (see eq. 4.14).

The group of events with the PGA varying from 18m/s^2 to 60 m/s^2 is modeled successfully using one set of the parameters. The waveforms of the first two impulses are well modeled with k_1 = 10,000-40,000 kN/m and damping constant β= 0.3. The remaining waveforms are modeled with k_1 varying from 80,000 to 120,000 KN/m , a damping constant ratio β= 0.6-0.8 and it is associated with a relatively small deformation of 1 mm measured at the center of support. The stiffness of the first part of the motion is much smaller than in the second part. Figure 4.7 shows the observed motion of the support in its middle and the theoretical motion. The first pulse was modeled using k_1 = 30,000 kN/m, β= 0.3 the rest of record was modeled using k_1=100,000 kN/m, the coefficient of damping ratio β =0.6. The inspection of Figure 4.7 shows that the theoretical support responses follow very closely the real velocity and have similar major features to the acceleration. The similar analyses of other examples of ground motion established that the good fit of the observed waveform with the theoretical is sustainable.

The question arises, why the stiffness of support and attenuation change during ground motion. The possible explanation could lie in the differing character of the ground motions of the hangingwall and footwall. The initial ground motion is out of phase (see Figure 3.6). The ground motion of the hangingwall strikes the support in the opposite direction to the strike of the ground motion of the footwall. The remaining part of the ground motion and the support motion has waveforms with synchronised phase. That feature of the stope motion is commonly observed during events at this site. The stiffness k_1 of the system is obtained in the center of the support with the assumption that the support is the SDOF system, it means, that the one k_1 is used to describe the whole support.

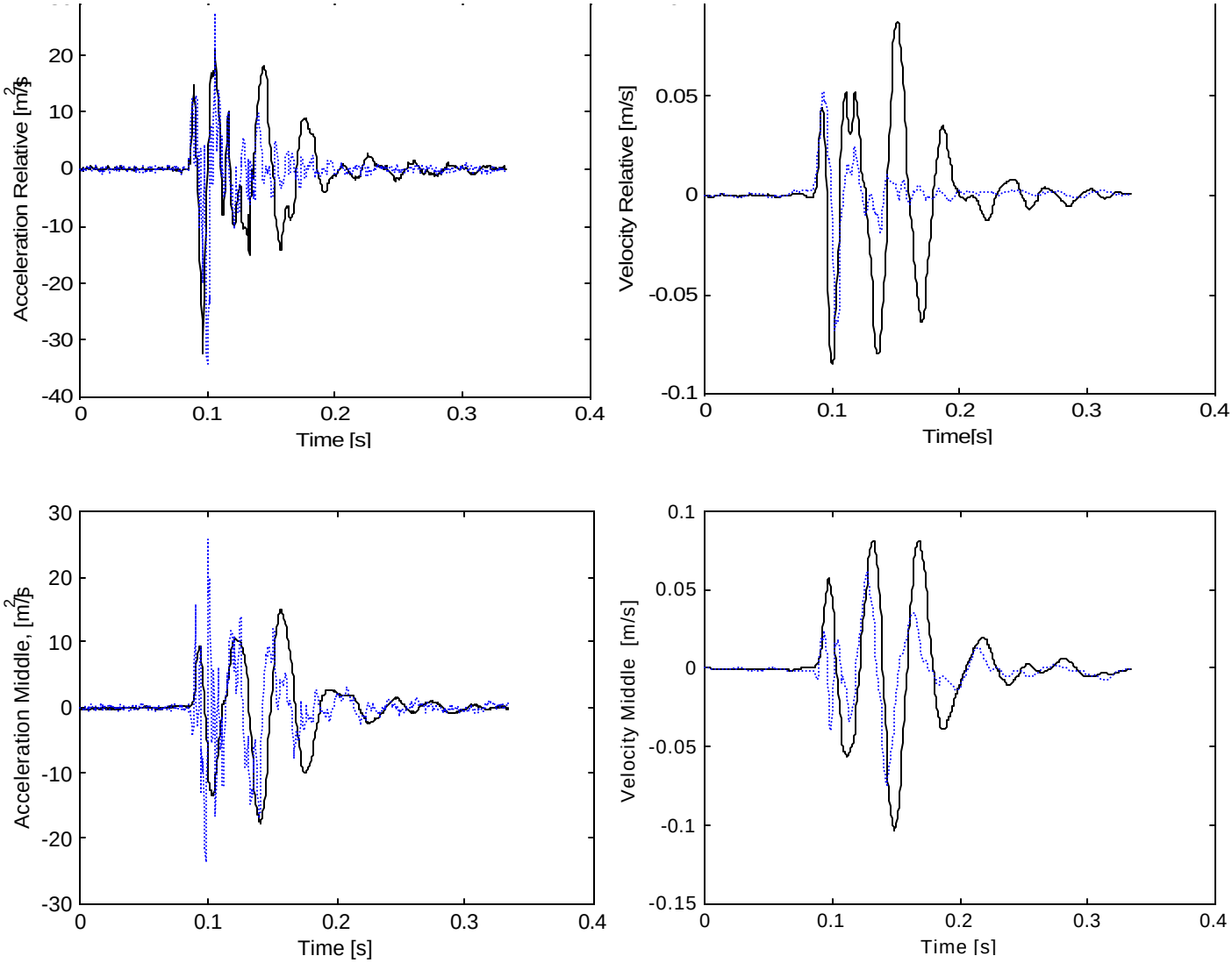

Figure 4.7 A Response of the timber pack to ground motion. The motion of the middle of the support ,$v_m(t)$, $a_m(t)$, and the relative motion of the middle of the support $v_r(t)$ $a_r(t)$ for the initial pulse and the whole waveforms are shown. The first pulse is modeled using k_1=30,000 kN/m, β= 0.3 The solid line represents theoretical acceleration and velocity, the dotted line is for the observed one. Data for the seismic event with magnitude 1.1 Mponeng Mine January,31, 2002, 00:02hr

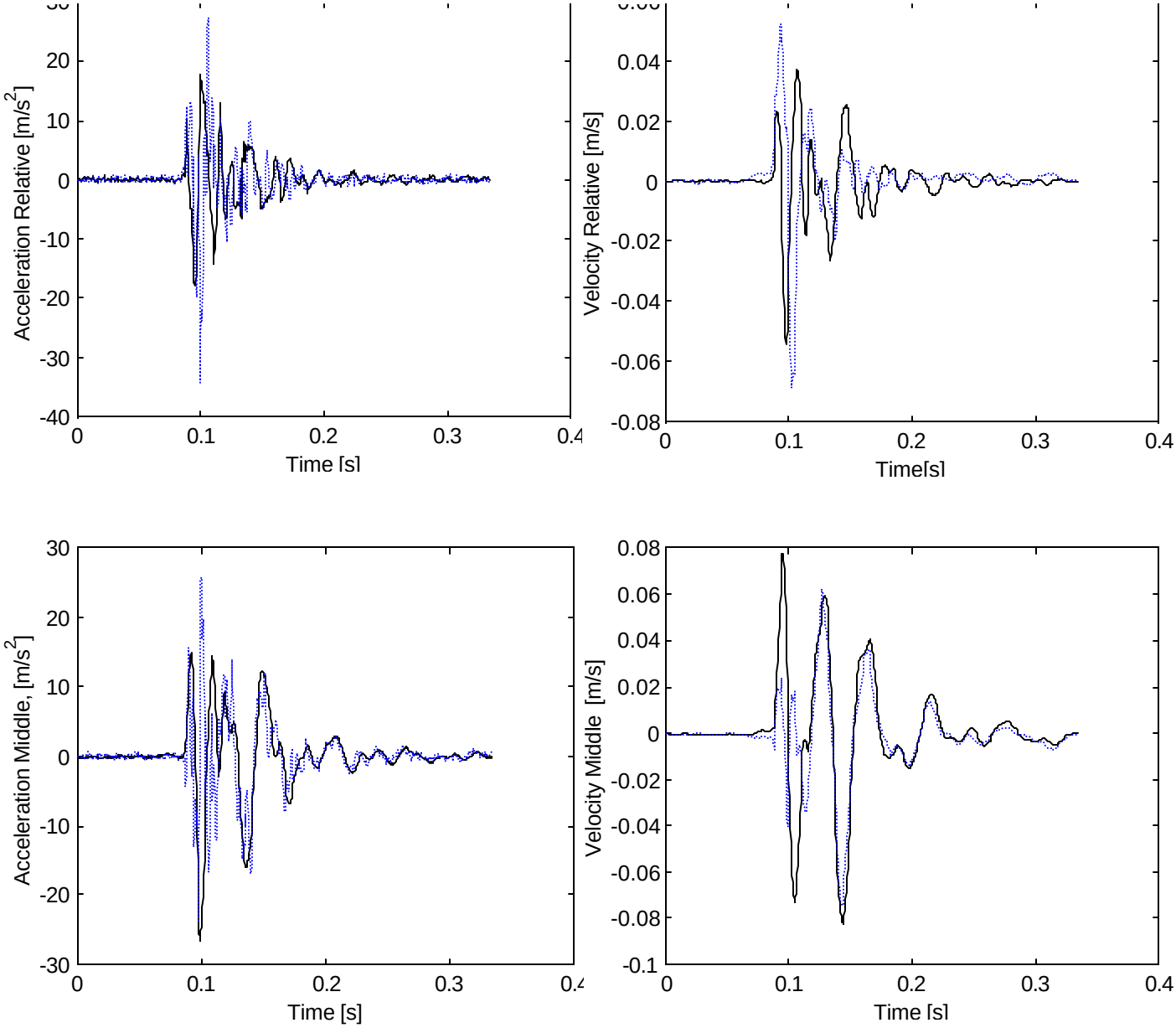

Figure 4.7 B The whole record is modeled using k_1=100,000 kN/m, β =0.6.

The strongest ground motion was caused by the excitation of the seismic event with magnitude 1.8 located above the stope (see Figure 3.7). Table 3.1 shows that the timber pack is deformed non-uniformly, therefore the SDOF model is not suitable for prediction of the support motion. A model with variable stiffness for the pack has to be used instead. However, the compressional response force acting on the support at the top may be obtained using equation 4.16. The deformation between the top and center of the support is 23.6 mm (see Table 3.1). The estimated support stiffness due to compression varies from 80 10^3 to 120 10^3 kN/m, and, consequently, restoring force, f_s, is 950-1400 kN.

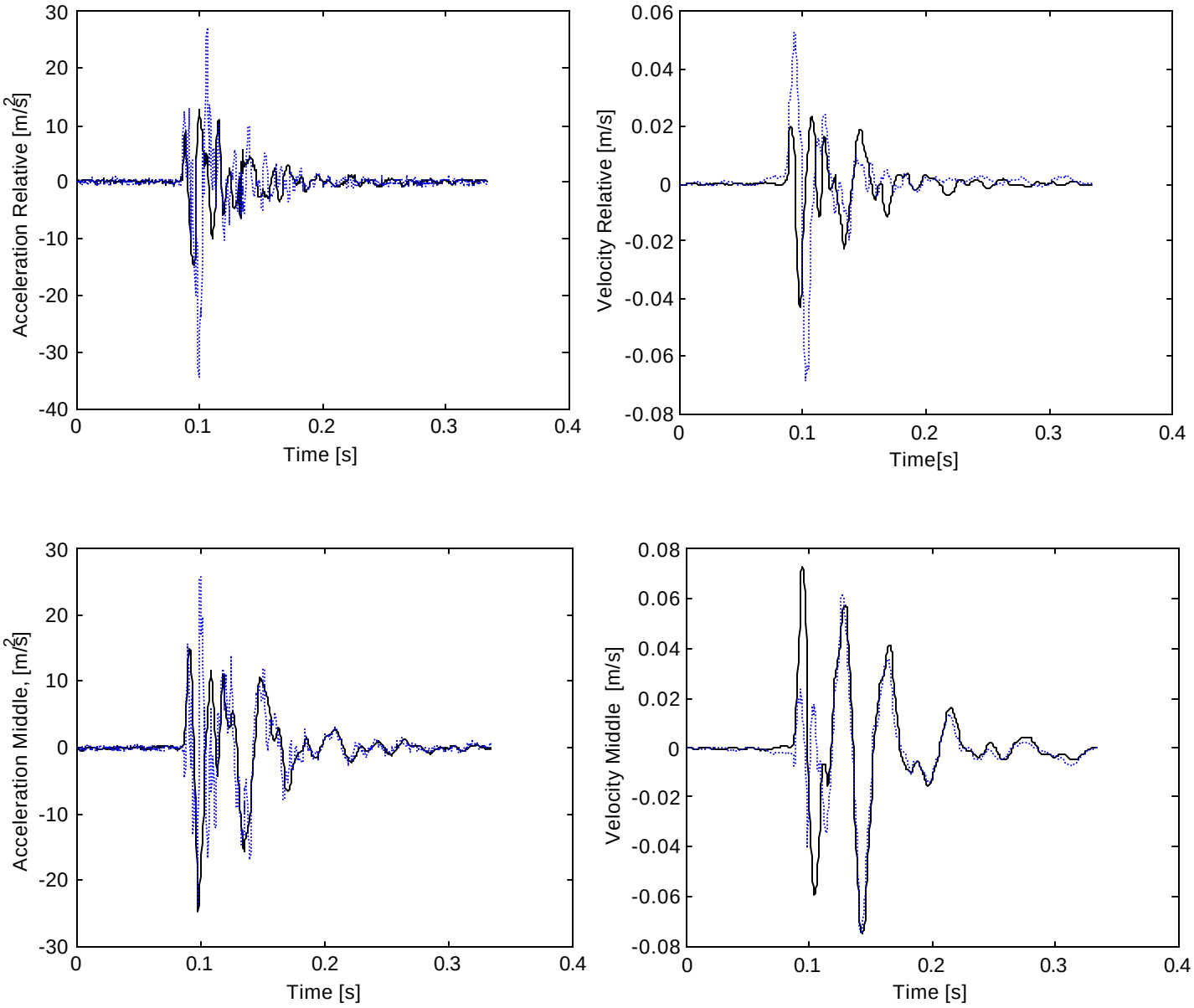

Figure 4.8 Response of the timber pack to the ground motion. The motion of the middle of the support , $v_m(t)$, $a_m(t)$, and the relative motion of the middle of the support $v_r(t)$ $a_r(t)$ for the whole waveforms are shown. The whole record is modeled using k_1=100,000 kN/m, β =0.8, f_y = 15000 N and stiffness after linear deformation, k_2=0.5 k_1. The solid black line represents a theoretical acceleration and velocity, the dotted line is for the observed ones.

The observed vibration of the support can be modeled as well using a non- elastic system. Figure 4.8 shows the observed and theoretical waveforms presented in similar fashion as in Figure 4.7. The theoretical waveform is obtained using k_1=100,000 kN/m, β =0.6, yielding deformation, f_y = 15,000 N and stiffness after linear deformation, k_2=0.5 k_1.

It is interesting to separately examine the restoring deformation force and damping force. Figure 4.9 shows the reaction force versus displacement and the reaction force plus damping force versus displacement for the event analyzed in Figure 4.7. The observed relationship shows, that f_s ($u_{r,,}v_r$) and $f_d(v_r)$ are not single -value functions. The figures display hysteresis loops for the restoring and damping forces. The areas within the hysteresis loop are equal to the energy dissipated by the support. The examples of the theoretical waveforms from Figure 4.7 and Figure 4.8 illustrate that the system can be simulated using different physical models. Information independent from observation has to be used to select the most likely model.

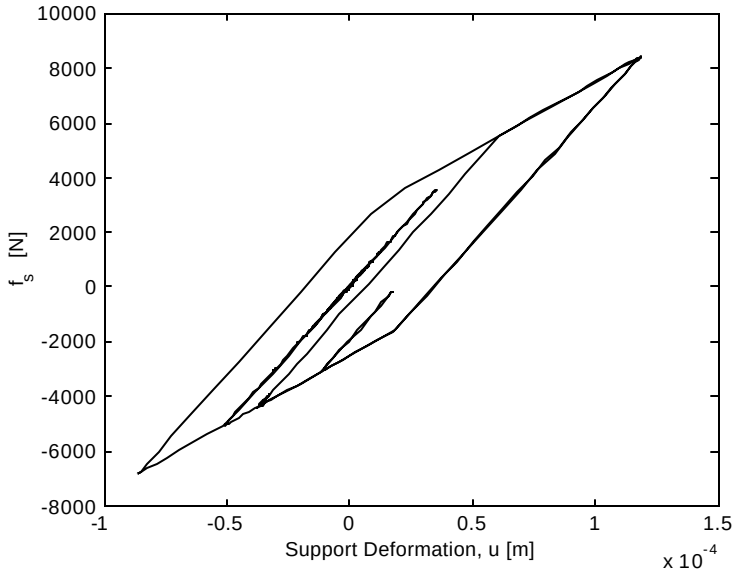

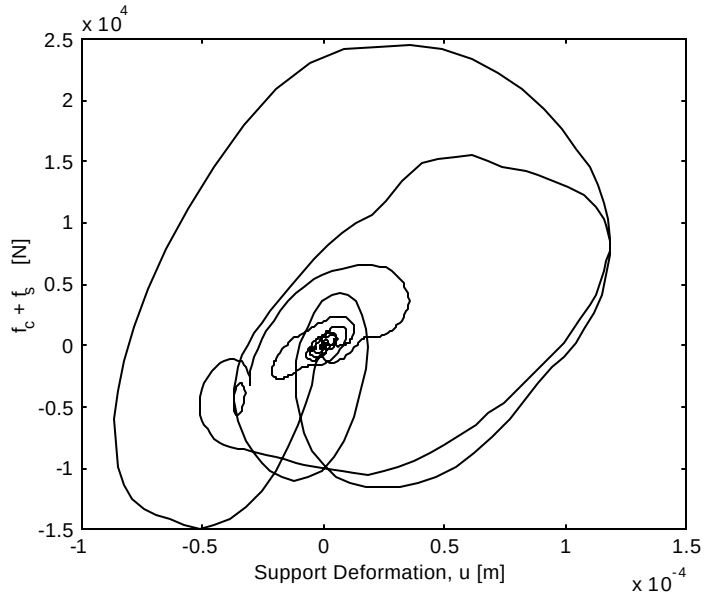

Figure 4.9.A The reaction force, $f_s(u_{r,,}v_r)$, versus displacement and the reaction force plus damping force, $f_s(u_{r,,}v_r) + f_d(v_r)$, versus displacement for the event analyzed in Figure 4.7. The whole record is modeled using k_1=100,000 kN/m, β =0.8, f_y = 15000 N and stiffness after linear deformation, k_2=0.5 k_1 Data for the seismic event with magnitude 1.1, Mponeng Mine January31, 2002, 00:02hr

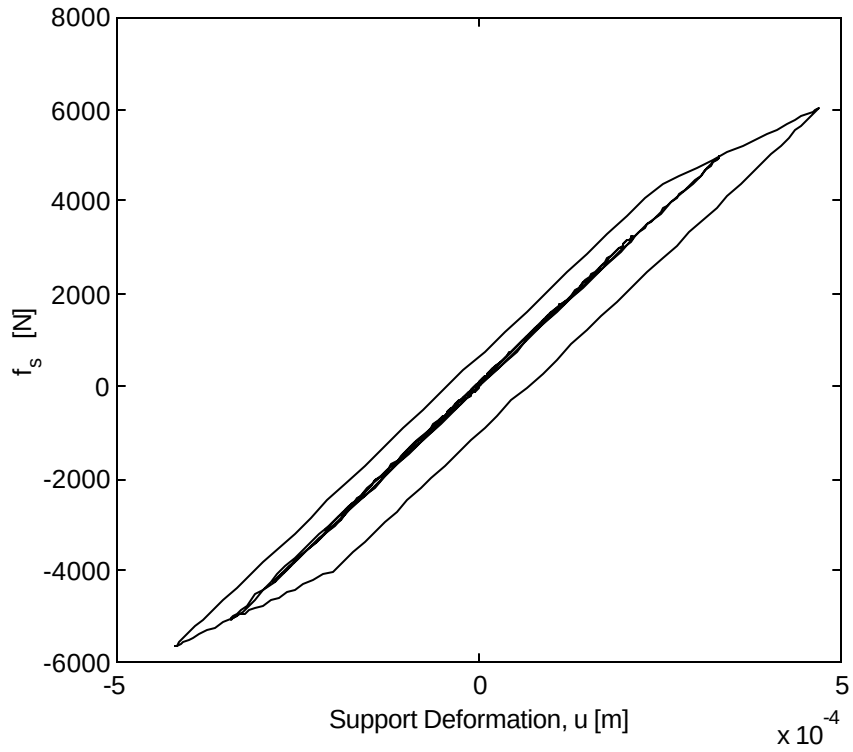

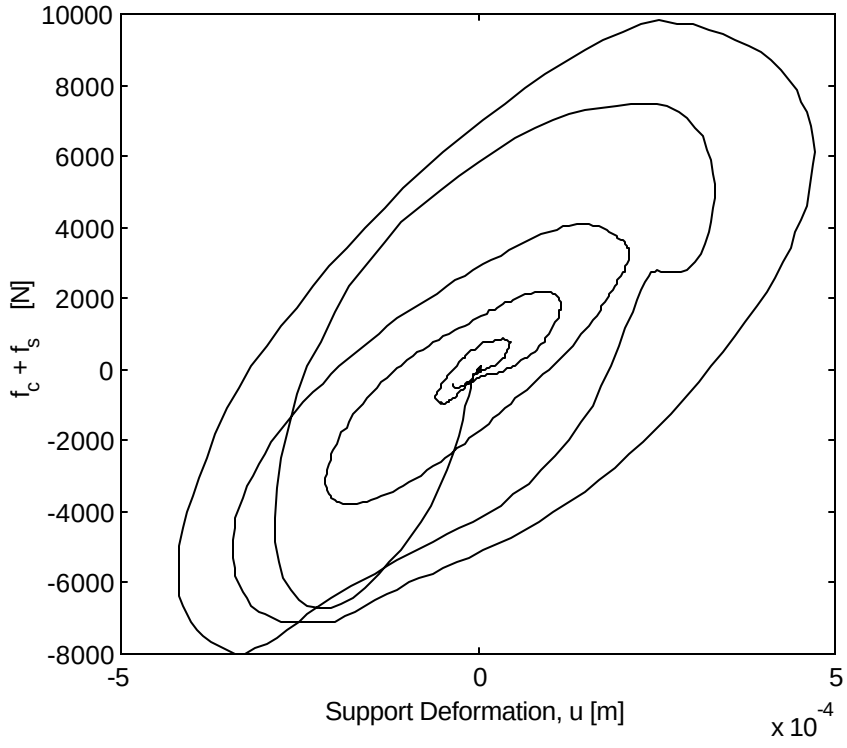

Figure 4.9.B The reaction force, f_s ($u_{r,,}v_r$), versus displacement and the reaction force plus damping force, f_s ($u_{r,,}v_r$) + $f_d(v_r)$, versus displacement for the event analyzed in Figure 4.7. The whole record is modeled using k_1=15,000 kN/m, β =0.3, f_y = 5000 N and stiffness after linear deformation, k_2=0.5 k_1 Data for the seismic event with magnitude 1.1, Mponeng Mine January31, 2002, 00:02hr

5 Energy balance in support during dynamic load

5.1 Estimation of energy absorbed by support units during strong ground motion

This report describes the theoretical basis for the estimation of energy absorbed by a support unit using data recorded in the support unit, hangingwall and footwall. The hysteresis energy dissipated by an inelastic structure, measures a cumulative damage by including the loading history of the seismic event. The problem of energy balance for an inelastic support unit is addressed. An energy balance equation shows how seismic energy imparted to support is distributed. The energy terms can be defined by integration of the equation of motion Eq. 4.18 with respect to displacement u_r

$$E_i = -\int_0^u m(\ddot{u}_h + \ddot{u}_f)/2\,du_r = \int_0^u m\ddot{u}_h\,du_r + \int_0^u c\dot{u}\,du_r + \int_0^u f_s(u_r,\dot{u}_r)\,du_r \qquad 5.1$$

where E_i is the total energy input to the structure. The integral can be taken with respect to time by using the relationship $du_r = v_r(t)\,dt$

$$E_i = -\int_0^T m(\ddot{u}_h + \ddot{u}_f)/2\,\dot{u}_r dt = \int_0^T m\ddot{u}_h\dot{u}_r\,dt + \int_0^T c\,\dot{u}_r{}^2\,dt + \int_0^T f_s(u_r,\dot{u}_r)\,\dot{u}_r dt \qquad 5.2$$

The first term on the right hand side represents the kinetic energy E_k , the second term represents the energy dissipated by viscous damping E_d and the third term represents the sum of the hysteretic energy E_h plus the strain energy E_s.

$$E_i = E_k + E_d + (E_h + E_s) \qquad 5.3$$

In the above equation energy is dissipated as damping, E_d, and inelastic, E_h, deformation and the remaining energy stored in the structure in the form of kinetic energy, E_k, and strain energy, E_s. The energy equilibrium on a structure subjected to a seismic ground motion is given by equation 5.3 The energy imparted to a structure is given by E_i .

A step by step numerical integration in the time domain will be used to calculate the various energy quantities. At first, the following quantities of support have to be estimated k_1,k_2,,α, c . (see Chapter 4.5) The energy time-history response of the structure will be used as a technique for classification of support response.

In the literature there is ongoing discussion about two types of energy method, based on relative and absolute formulations of the energy equation. Each approach starts from the equation of motion but leads to a different set of energy terms and its physical interpretation. This report follows the relative formulation because the kinetic energy represents the energy of motion relative to the base rather than due to the total motion.

Moreover, the energy dissipated in damping or yielding depends only on the relative motion. Therefore, the relative energy method seems to be a superior method for the purpose of this project. However, Bruneau and Wang (1996) argue that for a rectangular pulse, excitation is not base corrected, contrary to most earthquake records. The near field observation can be approximated with the rectangular pulse.

5.2 Data analysis

This section focuses on factors important in understanding the support response during seismic excitation and the amount of damage a structure may suffer. The energy imparted to a structure, the energy dissipated by damping and yielding deformation, kinetic energy and strain energy as a function of time are investigated. The most important aspect of the energy balance approach lies in the evaluation of the dissipated energy of the various structures.

Figure 5.1 shows the support response in the elastic range to the strong ground motion for seismic event with magnitude 1.1 on 1 January 31, 2002, 00:02hr. The support dissipates energy by viscous damping almost immediately. The damping process occurs almost from the beginning of the motion. The difference at any time between the curves for the energy input and the total energy dissipated represents the energy stored in the structure. At the end of the motion the energy imparted to the support is equal to the energy dissipated in the support.

The seismic input energy generally increases with time, but a local minimum occurs as some of the energy returns into the surrounding rock. The initial part of the ground motion has several impulses of kinetic energy and strain energy. It is apparent that the stored energy represents a small proportion of the energy imparted to the structure. The kinetic energy oscillates from zero, when the structure reaches its local maximum of deformation, to positive peaks, when the support passes through its undeformed position.

The energy is dissipated by viscous damping and yielding in the inelastic system (see Figure 5.2 A , B). The comparison of the Figure 5.1 with Figures 5.2 indicates that more damping energy is dissipated in the elastic system than in the inelastic one. The hysteresis energy grows when the damping energy diminishes . The numerical experiments show that the hysteresis energy is very sensitive to viscous damping. The energy dissipated by hysteretic action may reasonably correspond to the damage sustained by an inelastic structure. The values of the kinetic and strain energy are generally small compared to the damping and hysteretic energies at the end of the record. It is generally postulated that a structure can survive strong ground motion vibration, if the structure's energy absorption capacity is greater than the seismic input energy. Hysteretic energy, which is developed by inelastic action, can be considered as the seismic damage energy (Popov et al. 1995). If the dissipated hysteretic energy is very small, then an earthquake would cause little or no damage. Damage to a structure can be greatly reduced by using dissipaters. Various devices should be proposed to increase significantly the effective damping of the structure. Zahrah and Hall (1985) and Cruz and

Lopez (2000) have shown that extremely strong damping is responsible for the lack of yielding in the support structure.

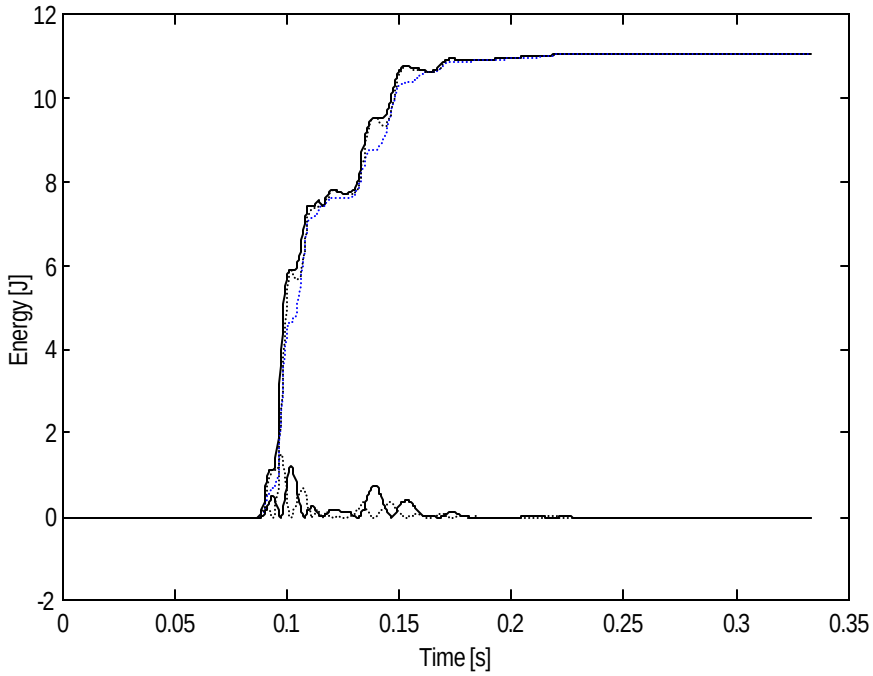

Figure 5.1 Time variation of energy dissipated by viscous damping,(top dotted curve) and kinetic(bottom dotted curve) plus strain energy(bottom solid curve),imparted energy (top solid curve).

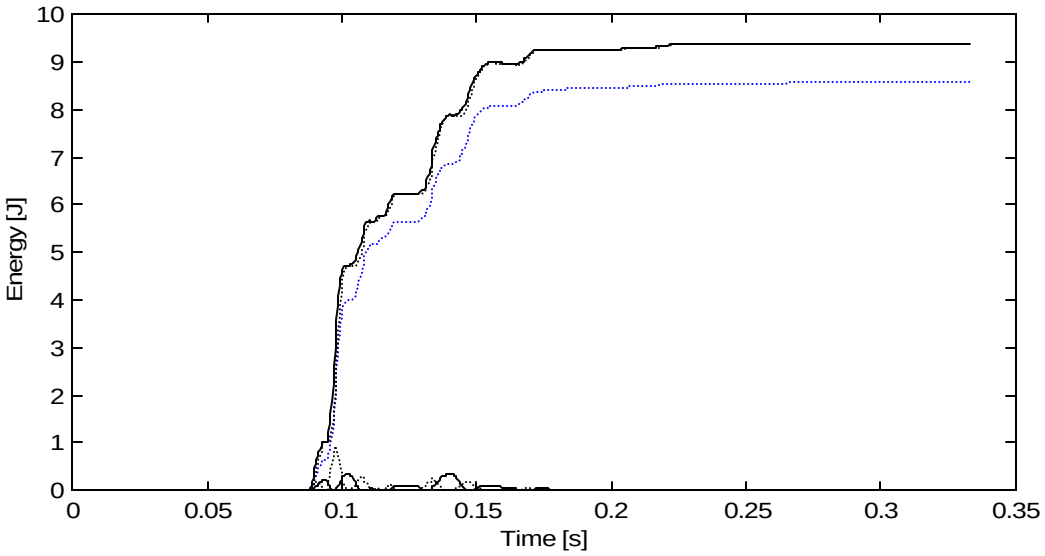

Figure 5.2 A Time variation of energy dissipated by viscous damping and yielding and kinetic plus strain energy, middle dotted curve - E_d. second dotted line, E_d,+$E_{h.,}$ top solid curve – $E_{i.}$ The whole record is modeled using k_1=100,000 kN/m, β =0.8, f_y = 15000 N and stiffness after linear deformation, k_2=0.5 k_1

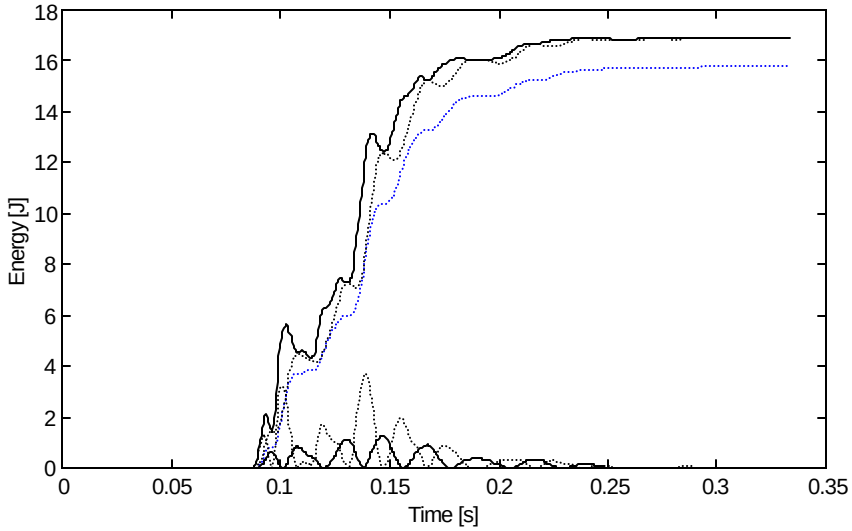

Figure 5.2 B Time variation of energy dissipated by viscous damping and yielding and kinetic plus strain energy, middle dotted curve - E_d. second dotted line, E_d,+$E_{h.,}$ top solid curve – $E_{i.}$ bottom dotted curve- $E_{k.,}$, bottom solid curve - $E_{s,}$.The whole record is modeled using k_1=15,000 kN/m, β =0.3, f_y = 5000 N and stiffness after linear deformation, k_2=0.5 k_1

6. Discussion

The purpose of this analysis is to provide the design engineer with a dynamical model of the stope support. The model has to describe the behavior of the stope support during strong ground motion. An adequate support model has to be able to predict the support motion caused by seismic load. The model of support is usually verified by comparing the observed support motion with the theoretical one.

The Handbook on Rock Engineering Practice for Tabular Hard Rock Mines, follows Wagner's equation (1984), that states that seismic input energy has to be absorbed by the support. The capacity of support to absorb energy is equal to the area under a load-displacement curve. This relationship correctly estimates a maximal possible displacement of support during a seismic event, however, it is not suitable for estimation of energy absorbed by support under a seismic load, as is claimed. The source of confusion starts when ground motion caused by a seismic event is understood as a monotonic dynamic load, so that it can be modelled, for example, using an experiment with a press. Seismic ground motion has a cyclic behaviour. This phenomenon comes as no surprise, although it is not considered by Wagner's equation.

Observed vibrations of the support show that some portion of impacted energy into the support will be dissipated as damping and inelastic deformation. This means that not the entire input energy is converted to permanent deformation. Therefore, the area under a load-deformation curve, calculated from zero to a value of maximal vertical displacement, does not measure the energy absorbed by support, because most of the input energy is returned to the surrounding rock. Energy absorbed by the support is mostly hysteretic energy. This statement has a very practical implication.

In earthquake engineering practice, damage indexes are used to describe a structure’s response to earthquake loading. The experience from past strong earthquakes has shown that the damage indexes should be based on the maximum deformation of the structure and the energy absorbed by the structure. The index of hysteretic energy has an advantage over ductility as a measure of cumulative damage, since it sums up the contribution from successive yield cycles, while ductility simply measures the peak displacement. Nevertheless, hysteretic energy demand is unable to distinguish between a sequence of low-amplitude yield cycles and a more damaging single deflection with high-amplitude with the same total energy. Several authors have proposed an index that includes both ductility and hysteretic energy.

This is a preliminary model of support response. The exact model of support response can be predicted using a system identification method. At least two records at different levels are needed, say the hangingwall and the footwall. To obtain such a model two real seismograms are used: an input signal, which is a seismogram recorded in the hangingwall or footwall and an output signal, which is a seismogram recorded in the support. These records normally contain the time history of the absolute acceleration, but can be used to generate the time history of the velocity and displacement as well. System

identification methods calculate parameters of a force-deformation curve for each cycle of the input signal in order to predict support response (output signal).

7 Conclusion

In this report it is assumed that the response of the stope support can be adequately simulated using a one-degree-of-freedom system. The SDOF model was developed for support under multiple excitations. Its advantages and limitations were verified by detailed testing with the strong ground motion data. The support may be modeled using SDOF approximately when PGA is in the range 18-60 m/s^2. The maximal value of the stiffness is 120,000 kN/m and it is associated with a relatively small deformation of 1 mm measured at the center of support. The strongest ground motion caused elastic deformation, however, a small inelastic component of the motion could be introduced as well.

The ground motion with PGV = 1.2 m/s is responsible for permanent deformation of 23.6 mm in the upper part of support and the maximal reaction force acting at the top of support is 950-1400 kN. The data show that the timber pack does not deform as one uniform block. The difference in ground motion between the hangingwall and footwall has an effect on the way the pack is deformed. The equation governing the model with two or three degrees of freedom with multiple excitation was developed.

The theoretical basis for the estimation of energy absorbed by a support unit using data recorded in the support unit, hangingwall and footwall was given. The damping and yielding influence the manner in which energy is dissipated. The energy is dissipated by viscous damping in the elastic system and by viscous damping and yielding in the inelastic system. The values of the kinetic and strain energy are generally small compared to the damping and hysteretic energies at the end of the record.

It is evident that the demand imposed on the support by strong ground motion is different to that imposed by weak ground motion. Therefore, parameters of weak ground motion cannot be used as an indicator of support behavior under strong ground motion as they are quantitatively different. A simple scaling law is not applicable. The peak ground velocity, PGV, or peak ground acceleration, PGA (converted to PGV), are not the best parameters for measuring the input energy to the support. The full waveform should be studied instead.

8. Recommendation for further research

The existing data should be further analysed. The simplified model should be extended to allow for variations of stiffness with change in time and space. The model with 2 or 3 degrees of freedom has to be solved as well. The research effort has to go toward producing the simplest possible model of support response but at the same time the major features of the dynamic response must be captured.

The collection of waveforms in the near field, where the sensor is 10-20 m behind the stope face is logistically a very difficult task. However, neither the existing laboratories nor PGV data collection can serve as a replacement for data which is obtained by strong ground motion sensors placed almost in the source area. Future experiments have to be able to collect the strong ground motion waveform together with a measurement of the dynamic displacement of the support.

References

Bruneau, M. and N. Wang, Some aspects of energy methods for the inelastic seismic response of ductile SDOF structures, Engineering Structure, vol 18, No1, pp1-12, 1996.

Cichowicz., A The meaningful use of peak particle velocity at excavation surface for the optimisation of the rockburst support criteria for tunnels and stopes SIMRAC Report GAP709b, 2001.

Chopra, A.K. Dynamic of Structure: Theory and application to earthquake engineering. Prentice_Hall, Englewood Cliffs, NJ 1995

Clough, R. W., and Penzien J., Dynamic of Structure, McGraw_Hill, New York, 1975.

Cruz, M. F. and O.A. Lopez, Plastic energy dissipated during an earthquake as a function of structural properties and ground motion characteristics. Engineering Structure, 22, 200, pp784-792.

Gupta .A.,K. Response spectrum method in seismic analysis and design of structure, CRC Press. Inc. 1995

Newmark, N.M., and Rosenblueth, E., Fundamentals of Earthquake Engineering, Prentice Hall, Englewood Cliffs, N.J., 1971

Michael Roberts (The design of stope support systems in South African gold and platinum mines, Ph.D. Thesis 2000

Popov E., P. C., E. Grigorian and T.,S. Yang, Developments in seismic structural analysis and design, Engineering Structure, vol, 17 no 3 pp187-197.

Zahran. T. F. and W.,j. Hall, Earthquake energy absorption in SDOF structures, Journal of Structural Engineering, vol 110,No 8 1984, 17571772.

Zembaty, Z., Spatial seismic coefficients, some sensitivity results, Journal of engineering mechanics, 1995, p 379-382.

Appendix 1 Seismograms

The strong ground motion data are presented in the order of the decreasing peak ground acceleration. The five sensors were installed at the surface of the hangingwall, in the top of the support, in the middle of the support, in the bottom of the support and at the surface of the footwall.

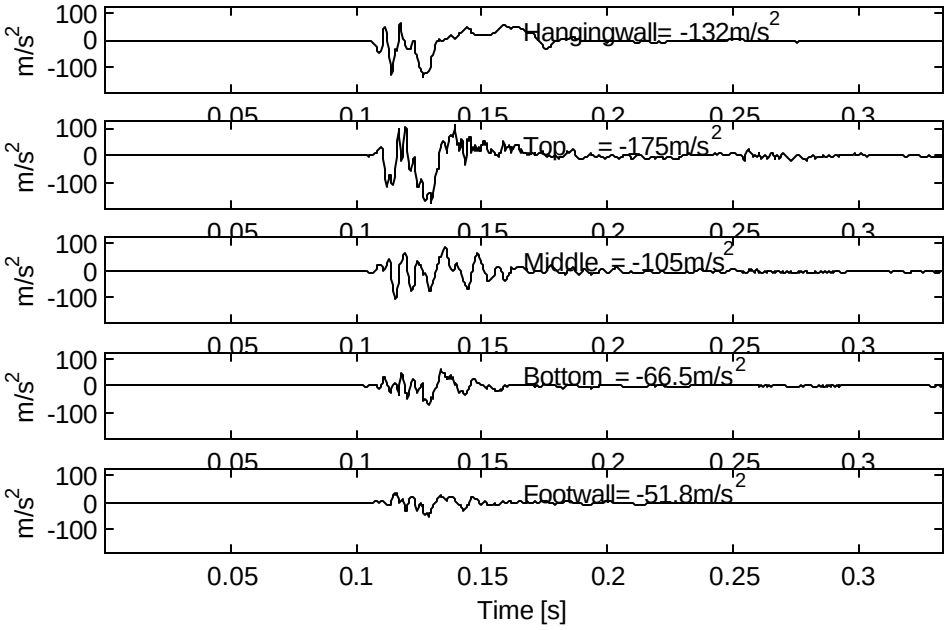

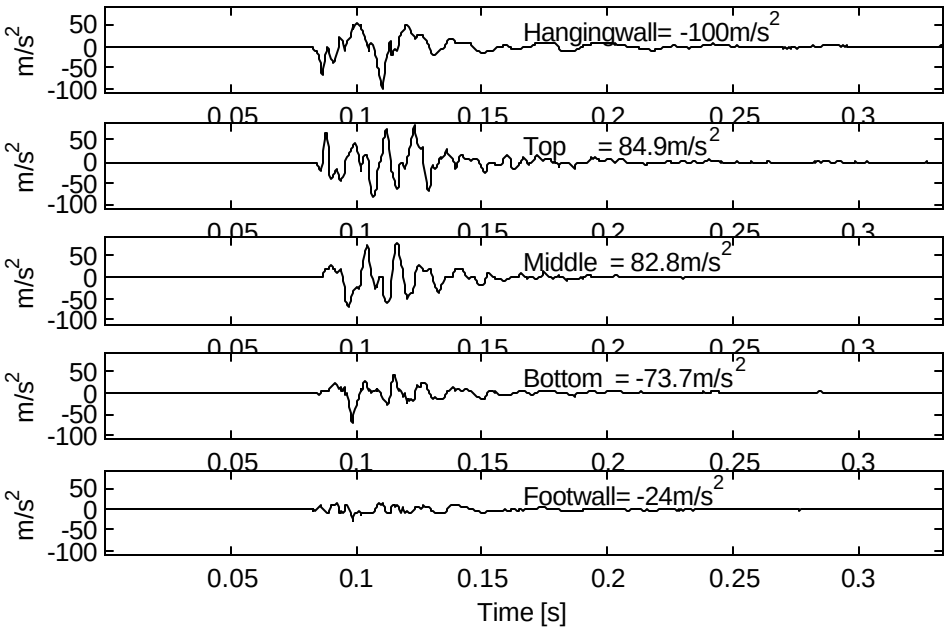

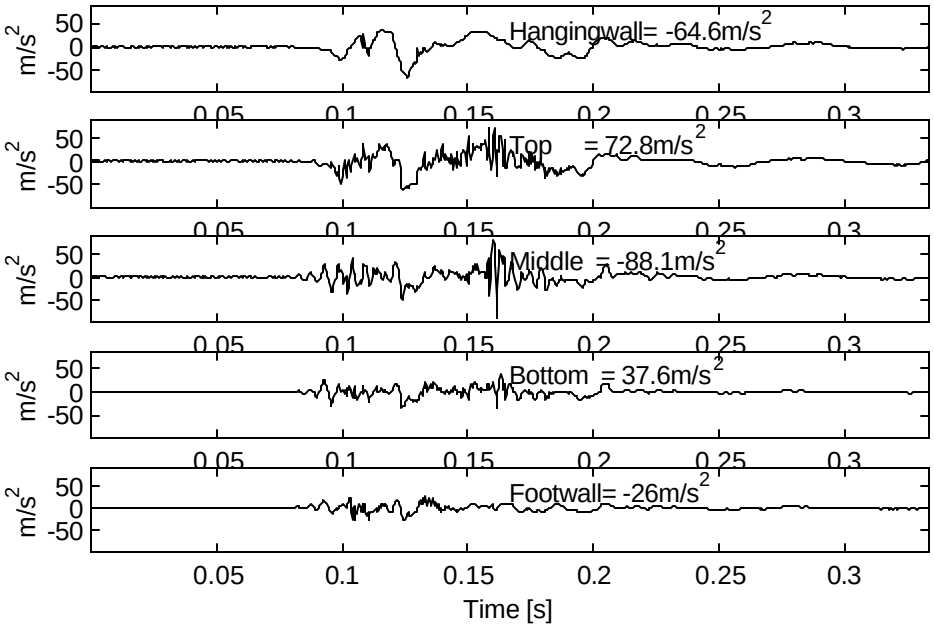
Hangingwall= -64.6m/s2
Top = 72.8m/s2
Middle = -88.1m/s2
Bottom = 37.6m/s2
Footwall= -26m/s2
m/s2
50
0
-50
0.05
0.1
0.15
0.2
0.25
0.3
Time [s]

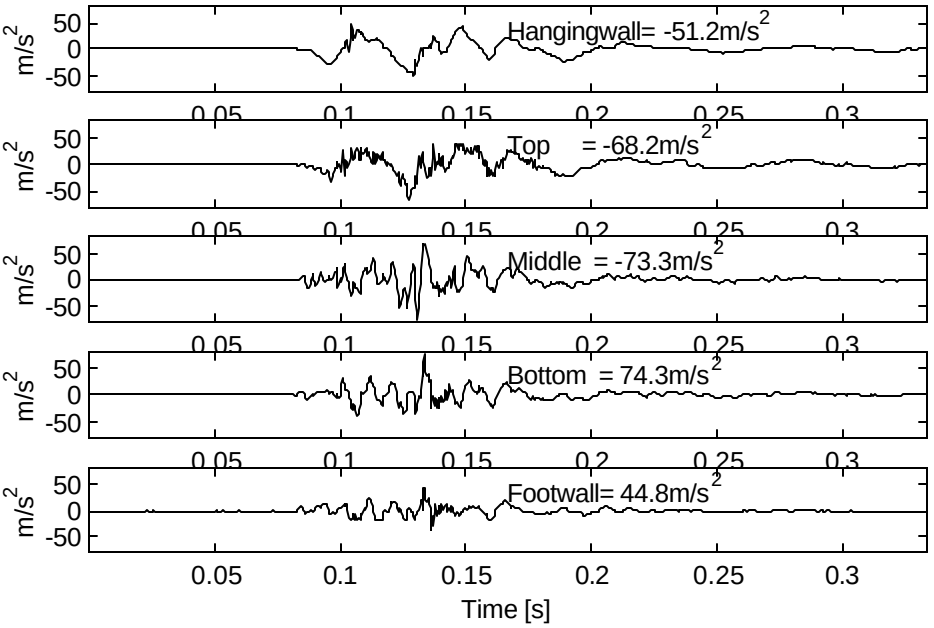
Hangingwall= -51.2m/s2
Top = -68.2m/s2
Middle = -73.3m/s2
Bottom = 74.3m/s2
Footwall= 44.8m/s2
m/s2
50
0
-50
0.05
0.1
0.15
0.2
0.25
0.3
Time [s]

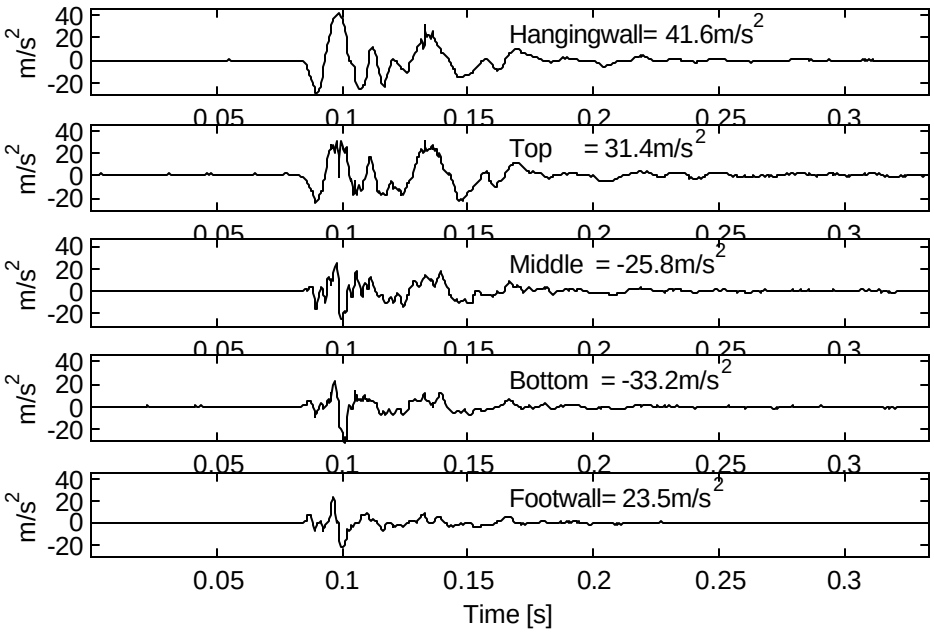
Hangingwall= 41.6m/s2
Top = 31.4m/s2
Middle = -25.8m/s2
Bottom = -33.2m/s2
Footwall= 23.5m/s2
m/s2
Time [s]

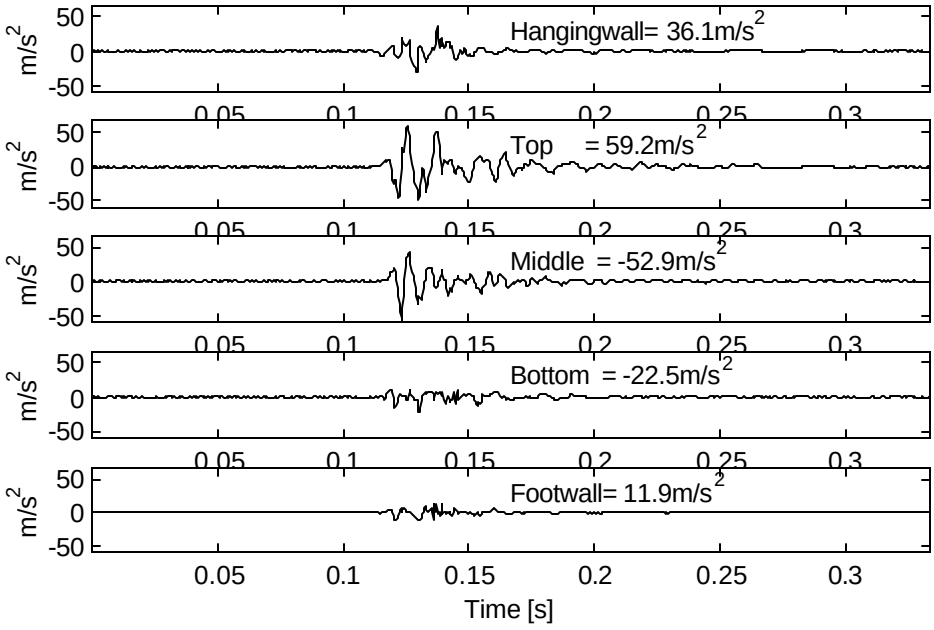
Hangingwall= 36.1m/s2
Top = 59.2m/s2
Middle = -52.9m/s2
Bottom = -22.5m/s2
Footwall= 11.9m/s2
m/s2
Time [s]

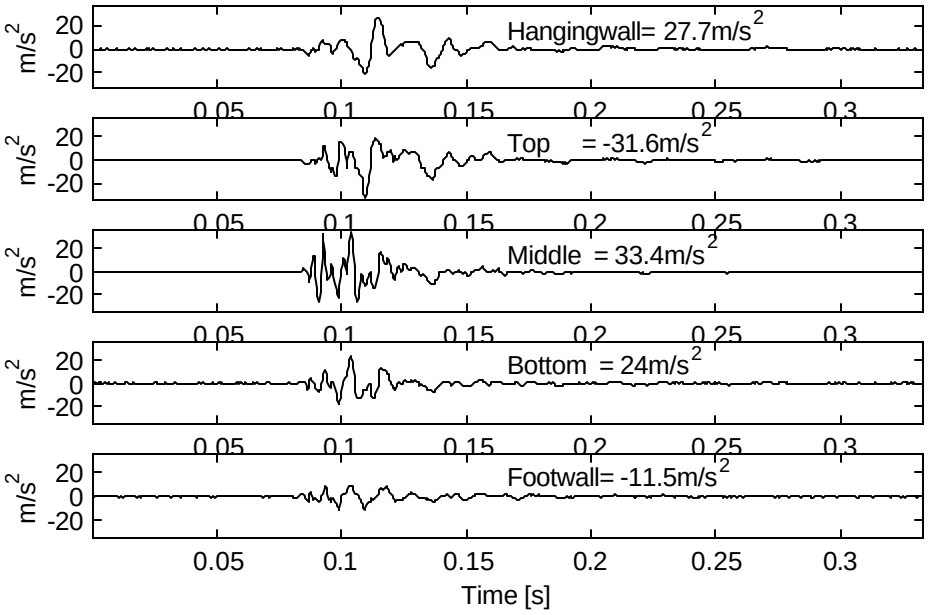
Hangingwall= 27.7m/s2
Top = -31.6m/s2
Middle = 33.4m/s2
Bottom = 24m/s2
Footwall= -11.5m/s2
m/s2
20
0
-20
0.05
0.1
0.15
0.2
0.25
0.3
Time [s]

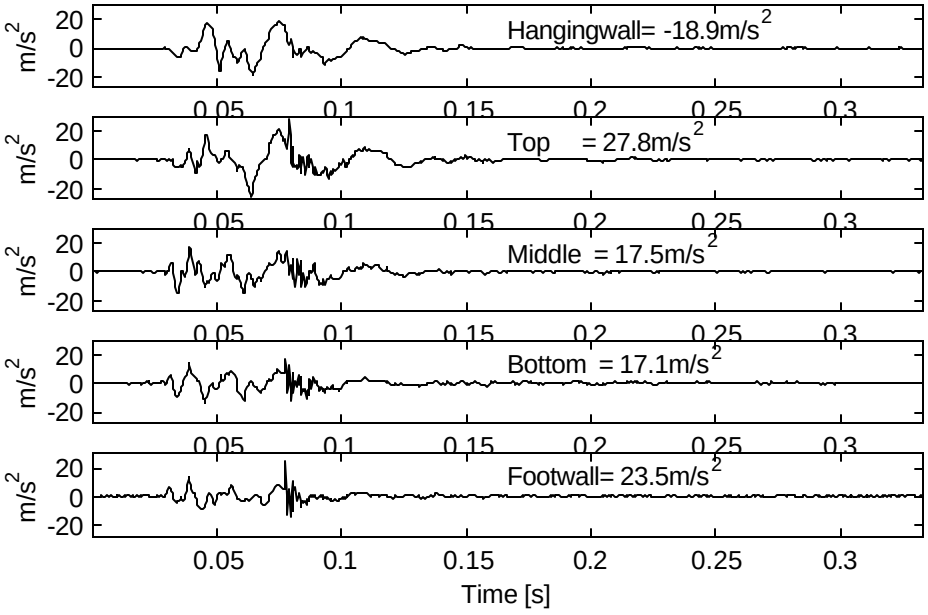
Hangingwall= -18.9m/s2
Top = 27.8m/s2
Middle = 17.5m/s2
Bottom = 17.1m/s2
Footwall= 23.5m/s2
m/s2
20
0
-20
0.05
0.1
0.15
0.2
0.25
0.3
Time [s]

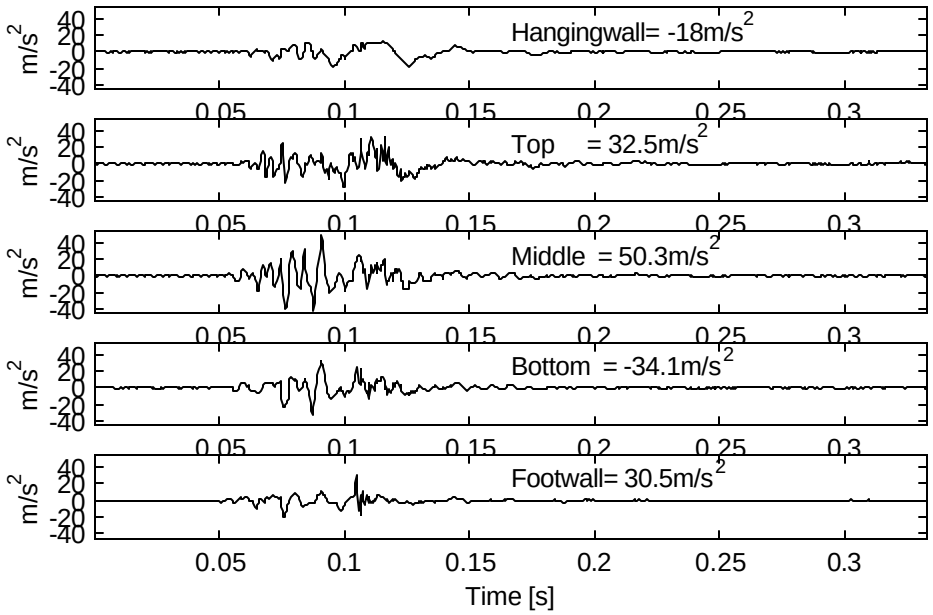
Hangingwall= -18m/s2
Top = 32.5m/s2
Middle = 50.3m/s2
Bottom = -34.1m/s2
Footwall= 30.5m/s2
m/s2
40
20
0
-20
-40
0.05
0.1
0.15
0.2
0.25
0.3
Time [s]

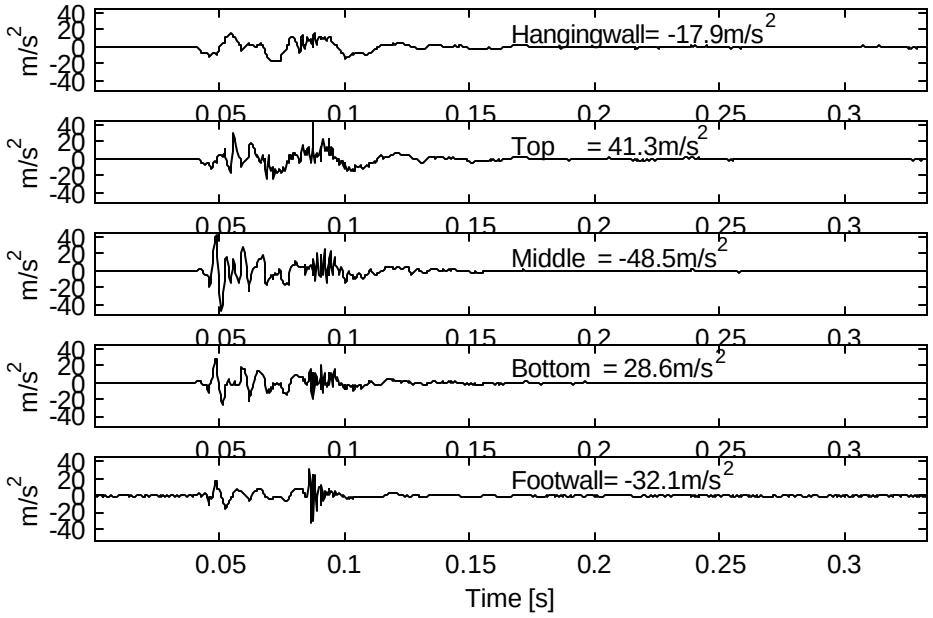
Hangingwall= -17.9m/s2
Top = 41.3m/s2
Middle = -48.5m/s2
Bottom = 28.6m/s2
Footwall= -32.1m/s2
m/s2
40
20
0
-20
-40
0.05
0.1
0.15
0.2
0.25
0.3
Time [s]

Appendix 2: Project Proposal

GAP 845
Project Proposal

Project GAP 845	Interaction between stope support and ground motion in the hangingwall and footwall.
Project Leader	Dr A Cichowicz (ISS International)
Duration	April 2001 to March 2002
Primary Output	The relationships between ground motion recorded in the hangingwall, footwall and stope support.
How Used?	The relationships will form the basis of a guideline for optimal rock burst support criteria.
By Whom?	Mine and Group Rock Mechanic Engineers.
Criteria For Use	Useful information for support design and damage potential.
Potential Impact	Optimal stope support.
Other Outputs	Enlarged database of strong ground motion measurements.

Enabling Output	**Enabling Output And Methodology**	**Milestone Dates**
	1. Data base of ground motion at the surfaces of stopes.	Dec. 2001
	1.1 A set of seismic instruments assembled for project GAP 709b to the value of R163,000 will be utilized. The recording instruments will be placed in a stope for a period of 7* months. Two units of three vertical components of acceleration (RSV3A) will be installed. The RS's are small and portable and a set of sensors can be installed in two to three days at any new selected site. During the experiment the instruments will follow the advancing face. (Continuation of GAP709b). *Consistent with the revised budget, the period of monitoring has been reduced from 9 to 7 months. This will effect the size of the database.	
	1.2 Maintenance of seismic instruments and building CD database (Continuation of GAP709b).	
	2. Stope support response to strong ground motion.	Mar. 2002
	2.1 Study of accelerogram waveforms recorded on footwall, hangingwall and support units. To understand phenomena of support damage under dynamic load the analysis will focus on strong ground motion with peak ground motion larger than 0.3 m/s. Two problems will be addressed : - Estimation of energy absorbed by support units during strong ground motion - Modelling of load deformation during cyclic seismic loading	

Motivation And Current Position	The data collection process for project GAP709b was sponsored for 5-6 months. The extension of the project would provide an additional 9 months of data collection.

A new set of data, collected during project GAP709b from Mponeng and East Driefontein Mines, provides new insight into the response of support units under seismic load. It is now clear that we should focus our research on a waveform of strong ground motion in order to understand the interaction between support and ground motion in the hangingwall and footwall.

The peak ground velocity, PGV, or peak ground acceleration, PGA (converted to PGV), are not the best parameters for measuring the input energy to support. They should especially not be used in a stage of research when one is trying to understand what happens in the support during seismic load. The full waveform should be studied instead. Available databases of in-stope ground motion measurements are dominated by records of weak ground motion. Such data is mostly useless as it does not carry information about damaging ground motion.

The Handbook on Rock Engineering Practice for Tabular Hard Rock Mines (1999), follows Wagner's equation (1984), that states, that seismic input energy has to be absorbed by support. The capacity of support to absorb energy is equal to the area under a load-displacement curve. This equation correctly estimates a maximal possible displacement of support during a seismic event. As support should not lose its integrity during a seismic event, this equation is essential to estimate a maximal possible vertical displacement (deformation).

Motivation And Current Position (Cont)

This equation, however, is not suitable to estimate energy absorbed by support under a seismic load as is claimed. A source of confusion starts when ground motion caused by a seismic event is understood as a constant dynamic load so that it can be modelled, for example, using an experiment with a press. The essential difference is that the seismic ground motion pushes support up and down. This phenomena is not surprising although it is not controlled by Wagner's equation.

Observed vibration of support suggests that some portion of impacted energy into support will be returned to the surrounding rock. This means, that the entire input energy is not being converted to permanent deformation. This statement has a very practical implication, however it has to be verified by more data.

Financial Details

	2000	**2001**
Project staff costs	395 000	
Operating costs	30 000	
Capital costs	20 000	
Collaborators	0	
Papers	10 000	
Sub Total	455 000	
Value Added Tax	64 000	
Total Project Cost	519 000	

Collaborators **Activity**

	519 000

Appendix 3: Statement on completion of the project GAP845 -chart

GAP845

July 2002

Task		15 July 2002
1	Data base of ground motion at the surface of stope	Completed
2	Stope support response to strong ground motion	Completed